JULY, 2018 M.Sc. in Aircraft and Aerospace Engineering DİDEM KINAY

UNIVERSITY OF GAZİANTEP

GRADUATE SCHOOL OF

NATURAL & APPLIED SCIENCES

EXPERIMENTAL INVESTIGATION ON MECHANICAL PROPERTIES OF ADHESIVELY BONDED AL-GFRP JOINTS REINFORCED WITH NANOPARTICLES

M.Sc. THESIS

IN

AIRCRAFT AND AEROSPACE ENGINEERING

BY

DİDEM KINAY

JULY 2018

Experimental Investigation on Mechanical Properties of Adhesively Bonded Al-GFRP Joints Reinforced with Nanoparticles

M.Sc. Thesis

In

Aircraft and Aerospace Engineering

University of Gaziantep

Supervisor

Assist. Prof. Dr. M. Veysel ÇAKIR

by

Didem KINAY

July 2018

REPUBLIC OF TURKEY
UNIVERSITY OF GAZİANTEP
GRADUATE SCHOOL OF NATURAL & APPLIED SCIENCES
AIRCRAFT AND AEROSPACE ENGINEERING

Name of the thesis : Experimental Investigation on Mechanical Properties of Adhesively Bonded Al-GFRP Joints Reinforced with Nanoparticles

Name of the student : Didem KINAY

Exam date : 26.07.2018

Approval of the Graduate School of Natural and Applied Sciences

Prof. Dr. Ahmet Necmeddin YAZICI

Director

I certify that this thesis satisfies all the requirements as a thesis for the degree of Master of Science.

Assist. Prof. Dr. M. Orkun ÖĞÜCÜ

Head of Department

This is to certify that we have read this thesis and that in our consensus opinion it is fully adequate, in scope and quality, as a thesis for the degree of Master of Science.

Assist. Prof. Dr. M. Veysel ÇAKIR

Supervisor

Examining Committee Members	Signature
1. Assoc. Prof. Dr. Ali Tolga BOZDANA	……..
2. Assist. Prof. Dr. Erdoğan KANCA	……..
3. Assist. Prof. Dr. Mehmet Veysel ÇAKIR	……..

I hereby declare that all information in this document has been obtained and presented in accordance with academic rules and ethical conduct. I also declare that, as required by these rules and conduct, I have fully cited and referenced all material and results that are not original to this work.

Didem KINAY

ABSTRACT

EXPERIMENTAL INVESTIGATION ON MECHANICAL PROPERTIES OF ADHESIVELY BONDED AL-GFRP JOINTS REINFORCED WITH NANOPARTICLES

KINAY, Didem

M.Sc. in Aircraft and Aerospace Eng.

Supervisor: Assist. Prof. Dr. Mehmet Veysel ÇAKIR

July 2018

83 pages

Aluminium and fibre reinforced polymers are widely used in the aerospace and automotive industries due to their high strength/weight ratios. While the use of adhesives in combination of different materials provides many advantages over mechanical methods, efforts are being made to increase the strength of the adhesive connection. In this study, the effects of adding Nano-particles such as Nano-silica, Nano-clay and multi-walled carbon Nano-tubes (MWCNT) to commercial epoxy adhesive (Araldite 2014) on the shear and impact strength of Al-GFRP single-lap joints were investigated. Shear performance of bonding samples were researched by universal tensile test machine in accordance to ASTM D 3039 international standards. In addition to this, Charpy impact test was used to evaluate the impact performances of samples in accordance to ISO 179 international standards. The experimental results showed that addition of Nano-particles give enhancements in the shear performance of Al-GFRP bonding joints by %38 to % 62. Impact strength is increased by 10% to 14%.

Key Words: Al-GFRP, Adhesive bonding, Nano-Clay, Nano-Silica, MWCNT, Shear strength, Charpy impact strength

ÖZET

NANOPARTİKÜLLER İLE GÜÇLENDİRİLMİŞ AL-GFRP YAPIŞTIRMA BAĞLANTILARININ MEKANİK ÖZELLİKLERİN DENEYSEL OLARAK İNCELENMESİ

KINAY, Didem

Yüksek Lisans Tezi, Uçak ve Uzay Müh. Bölümü

Tez Yöneticisi: Dr. Öğr. Üyesi Mehmet Veysel ÇAKIR

Temmuz 2018

83 sayfa

Al ve fiber takviyeli polimerler, yüksek mukavemet/ağırlık oranları nedeniyle havacılık ve otomotiv endüstrisinde yaygın olarak kullanılmaktadır. Farklı malzemelerin birleştirilmesinde yapıştırıcıların kullanılması mekanik yöntemlere göre pek çok avantaj sağlamakla birlikte, yapıştırıcı bağlantısının mukavemetini arttırmaya yönelik çalışmalar devam etmektedir. Bu tezde, ticari epoksi yapıştırıcıya (Araldite 2014) nano-silika, nano-kil ve çok duvarlı karbon nano-tüp (MWCNT) gibi nano-parçacıkların eklenmesinin Al-GFRP tek-bindirmeli yapışma derzlerinin kayma ve çarpma dayanımlarına etkileri araştırılmıştır. Yapıştırılan numunelerinin kayma dayanımları ASTM D 3039 uluslararası standartlara uygun olarak üniversal çekme test makinesi ile araştırılmıştır. Ayrıca, yapıştırılan bağlantıların darbe performanslarını ISO 179 uluslararası standartlara uygun olarak hazırlanıp Charpy darbe testi ile test edilmiştir. Deneysel çalışmaların sonuçları, yapıştırıcıya eklenen nano parçacıklarının Al-GFRP yapıştırma bağlantılarını kayma performansında %38 ila % 62 oranında iyileştirdiğini göstermiştir. Darbe dayanımlarının ise %10 ila %14 oranında arttığı görülmektedir.

Anahtar Kelimeler: Al-GFRP, Yapıştırma bağlantısı, Nano-Kil, Nano-Silika, MWCNT, Kayma Dayanımı, Charpy Darbe Dayanımı

for my dad

ACKNOWLEDGEMENTS

Firstly, I am very grateful to my supervisor Assist. Prof. Dr. M. Veysel ÇAKIR for teaching me almost everything I know about this research. I thank him for the patient guidance. He has taught me writing a thesis and paper over the last two years. From the initial recognition of my potential as a rising junior, through patient development of skills, he has helped me a lot to gain the confidence needed to be successful in research.

Secondly, I also forward my sincere thanks to in my thesis committee for their input and valuable comments.

Next, I would like to thank my dear friend, Professor Dr. Andreas Theo SCHERER, for helping me on the terrifying journey and encouraged me to start the MSc in Aeronautics Engineering. Thanks to him for each coffee conversation at Karlsruhe Institute of Technology's Mensa and his time which gave me to find myself academically, he constantly provided support and advice when I need it.

Next, I want to thank the people who have supervised me with my internship. Dear Dr. Ulrich GENGENBACH, as a group advisor, a role model, a comforter, a problem solver and a friend has great jokes. Besides, thanks a lot to Dr. Liane KOKER for her friendship. For any question, issue, or request, she was always there to provide advice and taught me how to do things down in the laboratory for my way in the internship.

Next, I must express Assoc. Prof. Dr. Murat ÇELİK. I have been extremely lucky to have a friend like him who cared about my thesis, and who responded to my questions. Also, I would like to thank my dear friend Dr. Andreas MELCHER for his guidance I have had to do for this thesis.

Next, I would like express my thanks Anna GRUBER for her friendship and helping with limitless conversations for troubleshoot with all of the roadblocks that come with all about of the study and business life. To her, for keeping me motivated and providing me strength and encouragement when I needed it the most in Germany.

Next, I extend my sincere thanks to all my friends for the continuous motivation and support.

I am also grateful to my bosses Selçuk BAYRAKTAR and Haluk BAYRAKTAR, for their understanding with days off for academic study, even though I am taking them during a busy season.

Last but not least, I want to thank my brother Gökhan KINAY for his unwavering support and belief in my abilities. Also, thanks my mom Nuray ÇAĞLAR. I would not have been where I am today and what I am today without my mom. Thanks to my step father Süleyman for keeping me grounded, always getting me to ask questions, and to look at things from a different angle. I know he is up there with my father, listening, watching over me and sending me his blessings constantly and is my guardian angel.

The most importantly, I would like to thank God for giving me the strength, knowledge, ability and opportunity to undertake this experimental-research study and to persevere and complete it satisfactorily.

Finally, I would like to acknowledge the support of University of Gaziantep with Research Project Management Unit with project number HUBF.YLT.17.02

TABLE OF CONTENTS

LIST OF TABLES

LIST OF FIGURES

CHAPTER 1

INTRODUCTION

Nowadays, different techniques and applications are used to combine many materials or constructs. The most common ones are riveting, welding, a method of bolted joints, and mechanically fastened. Specifically, looking at the aviation sector, it is clear how important it is to reduce fuel consumption and reduce the weight due to other circumstances related to its regulations. This view thus opens up the possibility of making connections with different methods, such as adhesively bonding joint technique. As a conclusion, the key point here is improving the strength of adhesively bonding joints and the work done in this direction.

1.1 Background

When considering joining and connections, the force and stress that affect the strength of the connection is distributed. Stress concentration accumulates in the joining areas and this affects the strength of the connection. For instance, if the riveting connections are taken into account, it is seen that the force is not evenly distributed. When adhesively bonding techniques are compared with riveting, it is seen that the bonding force distribution is more evenly spread. In addition to this advantage, when the results of the experiments and literature studies were examined, it was observed that the added nano-particles significantly increases the bonding connections. This thesis involves the experimental investigation of the increase in bonding quality and bonding strength when nano-particles added into adhesives.

1.2 Overview of the Thesis

When looking at the literature, it appears that nano-particles are being added to epoxy or polymer adhesives to study how they affect the mechanical properties of nano-composites or direct bulk adhesives. However, the mechanical relationships of the bonding connections and the degradation processes are very complex.

Moreover, the connection strength is affected by the type of adhesive, the length of the overlap, the thickness of the adhesive, and so on. In the studies carried out, it seems that fracture toughness in adhesive connections is also related to adherent materials.

Since adhesive joints are frequently subjected to sudden dynamic loads, information on how adhesive interconnects respond to impact loads, particularly those coupled to different materials, such as aluminium (Al) to Glass Fibre Reinforced Polymer (GFRP), is important. As a result, these effects need to be better understood by using different adherent materials and different type of adhesives and additives as nano-particles.

In this thesis, the adhesive bonding of Al to GFRP structure joints is investigated with single lap joint. It was shown that a commercial adhesive is made stronger with nano-particles.

First of all, a plan was done as shown in Figure 1.1. In numerical method it is necessary to know numerically the mechanical properties of the last state of the adhesive to make a correct analysis. Since it is not known how and in what way the adhesion strength of the nano-particles in the adhesive will affect, the numerical method is not considered in this plan. On the experimental path, the selection of adherents, adhesives, and nano-particles is required. Aluminium is already chosen as the adherent. Secondly, it is necessary to choose an aluminium alloy type. Thus, 3 different aluminium alloys were selected. The 1050 is an aluminium alloy, that is rarely found in the literature for single-lap joints, has high electrical conductivity, and can be used in various applications with GFRP in the future due to this feature. Aluminium alloy 7075-T6 and aluminium alloy 2024-T3 are frequently encountered in aerospace applications. Furthermore, two different commercial adhesives with different properties have been chosen as adhesives.

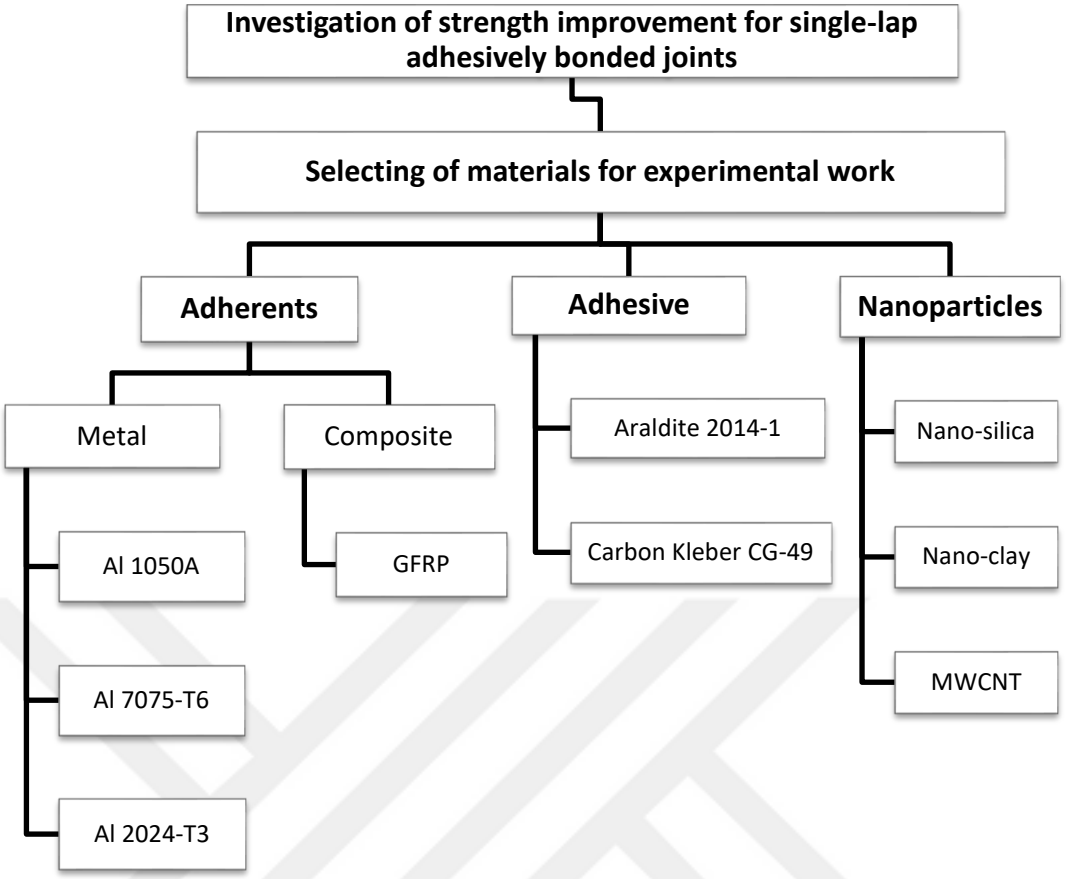

Figure 1.1 Plan of the experimental thesis

nano-silica, nano-clay and Multi-walled carbon nano-tubes (MWCNT) were selected as nano-particles (see Figure 1.1). In the thesis, Firstly Mode I experiments were conducted. Followings are mainly learned from it;

- Surface porosity quality in the adhesive bonding,
- Spew formation,
- Overlap area,
- Application method of adhesive,
- Experiences about adhesive applications,
- Weaker adhesive which is used rather than the other commercial one by tensile testing with ASTM D-3039 international standards.

Secondly investigation was continued with different adherents and nano-particles percentage in adhesive by weight. In Mode II tests, effect of the nano-particles adding into the adhesive with different percentage in weight was investigated.

Next, Mode III, IV and V tests are the field in which the dispersion formulation in the adhesive is understood and in which the mechanical properties of adhesives with different ratios are investigated. These cases were examined by single-lap joints and tensile tests were performed. Unlike the Mode III tests, in the Mode IV and V tests, adhesive joints were tested with ISO-179 international standards by Charpy impact tests.

Overall, 458 samples were prepared and 229 tests were carried out with tensile and Charpy impact tests in this thesis.

CHAPTER 2

LITERATURE SURVEY

2.1 Introduction

This section includes the literature review. Firstly, a review of the literature on adhesively joining and the related basic principles has been given in section 2.2. Then comes the single-lap joining, which is the connection method used. Next, literature review of Al to GFRP composite adhesively joining used in the experimental process was carried out. Later then, nano-particles as an overview and nano-particles specifically attached to the adhesive have been presented. Finally, tensile and Charpy impact tests have been mentioned in order to better understand which methods are used for the tests.

2.2 Adhesive Joining Fundamentals

Composite materials are widely used in the aviation and automotive industries as well as in construction and marine engineering fields. In many applications, it is almost impossible to complete the whole building in one single body. In this context, the integration of different parts has great importance.

Bolts or rivets are commonly used in composite and metal assemblies. Their assembly and disassembly processes can be done quite easily. However, when such applications are applied to composite materials, micro or macro damage may occur in the holes at the joining points. The adhesive joints, therefore, have advantages over the bolt and the rivet, and their use as alternatives to these assemblies are increasing.

Adhesives are, in a simple sense, fluid or semi-fluid liquids which adherent materials using surface or chemical bonds, either natural or synthetic. Adhesion is basically the atomic and molecular interaction between two surfaces [1].

Depending on the type of adhesive used, the bonding design, the application method and the intended function of the final system, bonding with the adhesive may offer one or more advantages. These are;

- Ability to combine different types of materials with different properties such as composition, the coefficient of expansion, elastic modulus, and thickness,
- Uneven surface lines caused by fasteners, such as bolts, rivets, etc., can be removed from the joint when joined with the adhesive to provide a permanent improvement in the appearance of the final system,
- A more uniform stress distribution along the entire bonding area can be obtained with the reduction of small stress buildups in small contact areas due to bonding elements such as bolts, rivets, and spot welds,
- Fretting (micro-movement of the parts running on each other) prevents corrosion,
- Prevents galvanized corrosion,
- Due to the tensile absorber, uniform distribution or advancement, the adhesive bonds of many adhesives provide higher strength and stretch elongation ability against dynamic impact. In this case, the fatigue strength improves and the vibration resilience and flexibility properties are improved,
- More precise rigid connections can be obtained,
- Provides lightness compared to welded and riveted connections when considering structural integrity,
- In the production of small forces and torques, it is possible to reduce machining costs, to use less material, and to work with higher tolerances [2, 3].

Along with these advantages of bonding joining, there are also benefits such as easy portability and combining different components together. The fact that the bonding processes can be easily automated makes it possible to make the bonding methods with this method convenient and low cost.

Compared with conventional joining methods, the combination of composite materials with other materials has become very popular due to its ease of application, low cost and light weight. They are also preferred for repairing damage to composite materials as they resist stress accumulation, are resistant to corrosion and have a long fatigue life. For this reason, it is frequently used in automotive industry and especially in the aviation sector [4-6]. For instance, the side walls of the aircraft and the honeycomb structures used for the covering are usually joined together by adhesives with aluminium plates [7].

Adams and Comyn [9] noted the importance of bonding connections and said that they are an alternative to the other joining techniques. Also, they emphasized that proper surface treatment and proper adhesive selection must be selected for bonding composite materials.

Lees et al. [10] focused on the issues to be considered in the bonding process. In addition, within this context, the chemistry of the adhesive has stated that the advantages and disadvantages of using adhesives, the length of overlap of the bonding, the effect of the thickness of the adhesive, and the appropriate loading shapes have to be determined. Also, the surface preparation methods of the most used engineering materials are emphasized.

Kinloch [11] has shown improvements in the use of adhesives, focusing on their use in composite materials for the automotive and aerospace industries. This study also explains the reasons for using adhesives and the factors that restrict their use, principally the rules to be considered, adhesion, cohesion, and curing.

In addition, Kinloch [12] published a paper titled "Adhesion and Adhesives" which explains the theories used in the description of the adhesion phenomenon and concludes that it is not enough to explain the adhesion phenomenon with a single theory. In this study, the preparation of the adhesion surface and the hardening mechanisms of the adhesives were given, and the mechanical behaviors of the adhesion bonds and the fracture mechanics were also explained.

Müller and his friends stressed out that bonded joint strength is a phenomenon that is technically affected by adhesion and cohesion [13].

Gediktaş [14] also described adhesion and cohesion in his study. He stated that the surfaces must be prepared appropriately in order for the bonding connection to be good, and adhesion forces and surface roughness at a bonding interface are the most important factors in transmitting force. It has been emphasized that the adhesive should not be very smooth and the surfaces must be roughened and this process can also be done with sandpaper. In addition, it has been emphasized that the surface should be prepared in various directions for sanding tracks.

2.3 Single-Lap Joint

Because of the fast development of adhesive bonding technology, adhesive joints are often used instead of earlier methods such as rivets in industry where aeronautics and space. Bulk of adhesively bonded joint configurations can be used in different bonding configurations. Because of its ease of preparation with basic principles, the single lap connection is the most common [15, 16].

Due to the fact that, AA2024-T3 has lightness, workability, high corrosion resistance, high strength, it is one of the important aluminium alloys used in the aviation and automotive industries. Use of this alloy is also recommended when evaluating the performance of many international standards adhesively joints [17].

In a study, Gültekin et al. [18] used AA2024-T3, which is widely used in aviation, and 3M-DP460, which is a commercial epoxy, as epoxy. For these single lap experiments, samples of different thicknesses were cut to 100mmx25mm size plates and for the 25mm overlap surfaces, 0.15mm thick adhesive was used. This experimental study is also modelled in ANSYS. As a conclusion, comparison of numerical and experimental results show good match. Also, transverse deflection indirect peel stress reduction in the overlap region with adherent thickness was observed in specimens from 1.6mm to 3.2 mm thickness. To sum up, this study showed that adherent thickness is an important parameter affecting joint strength.

In a study conducted by Reis and his friends [19], single lap joints' tensile shear strength was investigated using different materials. In this experimental study, 3 different materials were used and this study was investigated through the strengths of the materials.

The results of the experiments showed that the value of the stiffness of the materials affected the joints' shear strength. So it can be said that the strength in the joints can be related to the increase in stiffness.

Pinto and colleagues [20] studied single lap joints' tensile strength by using adhesives in ductile and brittle on using adherents of different thicknesses. One of the results of the experimental work is that joint strength is observed to decrease as the adherent thickness increases in the joint where the ductile adhesive is used. Another result is that the strength of the joint increases as the thickness of the adhesive increases as the brittle adhesive increases. These experiments have also shown that the adherents at different thicknesses reduce the joint strength.

Experiments conducted by Aydın et al. [21] focused on lap shear tests on single lap joints. Different adherent thicknesses and different overlap lengths have been studied. Also, the fracture surfaces on the specimens after fracture were examined with Scanning Electron Microscope (SEM). In addition, these tests were modelled in FEM according to non-linear material properties and run non-linearly. As a result of this study, the shear stress of the joint strength increased as the adherent thickness increased. The other result is the equal stress and strain transfer from the both ends of the bond to the centre of the overlap zone.

2.4 Metal to Composite Adhesive Joining

On one hand, fibre reinforced composite materials are far superior to metals in terms of specific strength, hardness, corrosion resistance and formability. On the other hand, metals are engineering materials that have high reliability and availability in almost any environment and are still important for large structures. For this reason, large structures such as airplanes and ships are made of metal and composites called hybrid structures [22]. Metal to composite based hybrid constructions are key technologies for high hardness, lightness, and reliability for other industries [23-27].

As mentioned before, there are two methods to combine metal to composite structures. These are mechanical fastening, which has been used for many years, and others that have been developed to a large extent in the last century.

The screwed and riveted joining technique from mechanical connections is a simple configuration, with no thickness restrictions and high performance with small connections possible. Hence, these connections are usually used in metal composite joining. However, mechanical connections have disadvantages a side form these advantages. The most important of these is the increase of the weight of the structure. This is a very serious disadvantage as weight is considered to be an important parameter in the aviation sector. In addition, the presence of holes in the mechanical connections causes static stresses due to stress build-up around the hole, resulting in damage to micro and macro dimensions.

Particularly in composite structures, when these holes are opened, the glass fibres break apart [28], the higher layer are peeled off at the entrance of the hole, the fibres are broken and the delamination of the final layers in the laminate occurs [29,30], so the overall structure of the composite material deteriorates. Since these damages can initiate fatigue cracks, they significantly reduce the strength of mechanical fastening.

2.5 Adhesive Bonding with Nano-Particles

Adhesive bonding is widely used in various industries such as aviation, automotive and ship due to its advantages such as lightness, sealing ability, low cost, corrosion resistance, and uniform stress distribution. Epoxy based adhesives, due to their mechanical, electrical, thermal and chemical properties are often used in engineering applications [31-33].

Increasing the quality and durability of adhesives using various methods is a hot topic both in science and engineering. These methods include the use of nano-particles such as nano-fibres, carbon nano-tubes and graphite. As well as the method's practical and low cost, mechanical, thermal and permeability of epoxy adhesives offer promising developments in an adhesive's properties. Studies have shown that the addition of various low concentration nano-particles to the resins of polymer composites is a good solution to improve mechanical and impact performance without sacrificing toughness or manufacturing process. For instance, Chavooshiana et al. [35] conducted a study on the effect of silicon carbide nano-particles on adhesion strength of glass fibre composite links bonded with two-component structural acrylic adhesives. They have reported that the use of nano-

silicon carbide particles in this work resulted in a significant increase in the shear and tensile strength of the composite connections.

2.6 MWCNT in Adhesive

Zielecki et al. [36] aimed at improving the fatigue properties of the adhesive with MWCNT (30 nm diameter, few microns length) and experimentally applied the peel loaded adhesive joints method. In these tests, 3 differently varied tests were applied, 3 different types of epoxy were used for each variation and it was planned to apply the same test for each adhesive. In this literature review, the authors found that the most effective results were achieved with adhesives containing 1% by weight of additives. Therefore, they used only 1 wt. % MWCNT nano-particles in their tests. For these tests, the epoxy was heated to 50 °C to reduce the viscosity. Subsequently, the nano-particles were added with epoxies and mechanically mixed with ultrasonic bath before homogenous dispersing was provided. The fatigue strength test results showed that the fatigue life improved significantly. Fatigue life at the connections with Epidian 57-PAC adhesive and MWCNT particles was 106.8%, fatigue life at the connections with Bison named adhesive and MWCNT mixture increased by 69.3%.

In addition to that, the fatigue strength was 19.5 MPa at neat Epidian 57. Then, it increased to 22 MPa at MWCNT adhesive. On the other hand, it increased from 12.2 MPa in neat Bison to 13.5 MPa. Araldite 2014-1 is a named adhesive it does not give a good result as compared to the other adhesives. The authors explain the reason for these successful results by increasing the energy absorption of MWCNT, and they believe that such adhesives will be widely used in the future because of the increased strength properties of bonded structural joints.

A study by Zhang et al. [37] found that C/C is frequently used in aeronautic and astronautic fields due to its heat resistance feature, but due to their complex shapes and sizes they cannot be used directly and they are used by being combined with high-temperature resistant adhesives. On the other hand, they stressed the knowledge that these adhesives have low mechanical properties even if they are resistant to high temperatures. Therefore, in this study, which aimed to increase the strength and stiffness of the C/C adhesive joining, the adhesive was mixed with 0.2 wt. %

MWCNT (8-15 nm diameter, 50-micron length) particles. Compared to neat epoxy, the stiffness is much higher. An increase in average shear strength of 27% to 31% is achieved. In addition, it is emphasized that MWCNT provides strong interfacial bonding in the matrix and stress transfer is high.

Yu et al. [38] investigated the effects of MWCNT (20 nm diameter, few microns length) additives on the adhesive connections of aluminium plates (150mm×25mm×3.2mm).

For the tests, MWCNTs in different percentages were determined and the homogeneous dispersion, electrical and thermal properties of the adhesive was mainly investigated. This research, unlike other researchers, investigated dispersion as follows; The CNTs were first mixed with a hardener (Epicure 3274) and an ultrasonic bath was first used after mechanical stirring to ensure good dispersing. On the other hand, the CNTs were also mixed directly with the epoxy (Epikote 240) and as a result, a poor dispersion was observed. To increase the quality, the mixture was mixed again with a high-speed beater, but this time the bubbles appeared in the mixture. The adhesive was placed in a vacuum oven to remove bubbles, but removal was difficult.

Tests were carried out with the Boeing wedge test method and neat and CNT samples were immersed in water at 60 °C. As a result, under these conditions, while samples with neat epoxy failed, the samples of 1% CNT still showed fracture toughness under the same test conditions. However, the electrical properties of the adhesive have been studied. Despite being a very good insulating material when the epoxy is on its own, it has an epoxy semi-metallic / metallic feature with CNT. That is, the addition of CNT increases the electrical conductivity.

2.7 Nano-Silica Particles in Adhesive

When examining the work of adding nano-silica, Tutunchi et al. [45] reported a significant increase in the addition of 1.5% by weight of nano-silica particles to the shear and tensile strengths of steel glass fibre connections bonded with two component acrylic adhesives.

Meng et al. [49] mentioned that high performance adhesives are found in many applications and therefore added 2.1 % by volume nano-silica (20.3±3.1 nm) to develop a commercial adhesive. They explained that with this addition, they increased the fracture toughness of the epoxy to 605%. In addition, nano-particles have a higher toughening adhesive effect than the particles on the micron size.

Zhou et al. [50] studied nano-silica in their research. They mentioned that epoxies are used in many engineering disciplines and therefore need to be improved. In the study, 10-20wt. % nano-silica added to epoxy. Adherends were made of stainless steel materials, and single lap joint's tensile tests were performed. With this additive contribution, joints strenght increased by 20%. In addition, surface morphology was examined by SEM. To sum up, when the cyclic fatigue test is performed, it is concluded that the adhesive has a longer life time than the neat epoxy.

2.8 Nano-Clay Particles in Adhesive

Recently polymeric clay nano-composite (PCN) has been academically and industrially intriguing because of its strong impact between polymer and silicate platelets, as well as the dramatic increase in mechanical and thermal properties of molecules and low clay content on nanometer scale [51]. Montmorillonite nano-clay particles; polymer nano-composites have been documented as the best reinforcing materials because of their high aspect ratio, low cost and the formation of layered silicates that can be placed in nano-dimensions separately with polymer chains [52]. Khalili et al. [53] have investigated the mechanical properties of glass fibre composite to composite's single bond connections combined with the nano-clay addition to the epoxy adhesive under static and dynamic loading in a study they performed, as a result, 1 wt. % of the nano-clay particles showed maximum strength at tensile load.

Although studies on these new nano-composites called PCN are common, there are a limited number of studies on the effect of nano-clay addition to the adhesive when plate-like materials are combined with adhesive. In addition, it is observed that the adhesive materials are generally uniform.

Khalili et al. [53] in their study, they added nano-clay particles to 1, 3 and 5% epoxy adhesive (Araldite LY5052) by weight. The assemblies were subjected to in-plane

and out-of-plane Charpy impact tests. The results show that adhesive joints with 1% nano-clay particles have the maximum strength in tensile load and those with the highest Charpy impact energy have bonded joints with 3% nano-clay particles.

Reis et al. [54] have added mushroom powder and nano-clay to epoxy resin to improve impact behaviour of Kevlar/epoxy composite sheets. It has been shown that the increase in impact energy in composite plates due to filler material and nano-clay particle addition show better performance in terms of impact behaviour compared to mushroom powder.

Rafik et al. [55] investigated the effect of Nano-clay addition on glass fibre reinforced composites on impact response. They have shown that up to 3% by weight of nano-clay addition improves impact resistance while 1.5% by weight of Nano-clay addition is at an optimum level with an improvement of 23% at impact peak load and an increase of 11% in hardness.

Jeyekumar et al. [56] have produced glass fibre composites using 1, 3, 5, 7% nano-clay by weight. They pay attention to homogeny dispersion and observe it in SEM. The samples were subjected to tensile and impact tests. With results of 5% additive order; tensile strength and modulus 23.66%, flexural strength and modulus 53.86%, impact strength 29.65%.

Galimberti et al. [57] have investigated mechanical, barrier and thermal properties of composites produced using nano-clay in a study they have done. In addition, it has been shown that the nano-clay minerals increase the glass temperature (Tg) of the adhesive.

2.9 Tensile Testing

Bonding connections used to combine different types of materials; designers offer significant advantages in terms of low number of parts used, light weight, installation time, stress accumulation, sealing, cost, improved fatigue and corrosion resistance, smoothness and aesthetics.

Epoxy adhesives are adhesives with excellent chemical and corrosion resistance as well as high mechanical and thermal properties. However, such adhesives have poor resistance to low fracture toughness and hence high crack formation due to their

cross-linked structures. Micro fractures can cause disruption in service, resulting in vibrations, weather conditions, or unexpected disaster.

Mechanical connections and degradation processes of adhesive connections are typically very complex. The type of adhesive, the type of adherent materials, the overlap, and the thickness of the adhesive affect strength of the connection. Therefore, these effects need to be better understood by using different materials and different adhesives by tensile testing [58].

In this thesis, a total of 129 tests were carried out with a universal testing machine Shimadzu AG-X with a capacity of 300 kN in accordance with ASTM D 3039 standards.

2.10 Charpy Impact Test

Epoxy adhesives; can be said to be the most widely used structural adhesives because of their good mechanical, thermal and chemical properties [59]. Such adhesives are frequently preferred in the aerospace, automotive and naval sectors. These adhesives also generally have low fracture toughness. In an airplane, structural parts are subjected to various unanticipated impact loads during operation. On the other hand, in the automotive industry, it is very important to transfer the load to the body under impact load without damaging the body, thus ensuring the integrity of the car in the event of collusion [60].

High strength materials such as aluminium and steel have been replaced by laminated fibre reinforced composite materials with higher strength values in some applications. As with all air vehicles, the use of composite materials is especially important in high-speed aircraft because they are lightweight, durable and useful for many applications in aeronautics. But these materials are very susceptible to impact damage. Therefore, the impact tests are important for composite materials and/or bonded composite materials with metals.

Impact resistance of a material is defined as the energy required for fracture along the unit cross section during high-velocity loading. It is a measure of the ability of the material to withstand the impact force.

The addition of nano-particles to the adhesive generally increases their mechanical strength, which in turn increases the fracture toughness of the nano-particle depletion without losing its inherent cohesive properties.

In this thesis, 10 different types of samples were prepared for each ratio of nano-particles according to the ISO 179 standard using a Kögel 3/70 Charpy impact tester equipped with a 15 J hammer. Besides, a total of 100 tests were carried out. In the impact test, the energy absorbed during fracture is used as a measure of the brittleness or impact resistance of the material.

Hsieh and Liang [46] have worked with nano-fibres and nano-silica in their work. These particles are added to the epoxy used to make the carbon fibre composite material. Besides, they have examined the surface morphology with SEM. As a result, impact absorption energy increased by 11% in nano-fillers used at 0.2% by weight, and 8.7% at 0.1% used nano-silica.

Nassar et al. [47] investigated the force carrying capacity by adding silica and alumina nano-particles to the single lap of magnesium to steel adhesive bonding. Experimental results have shown that silica particles increase the force carrying capacity of the joining when compared to alumina particles.

Zhou et al. [48] investigated the shear strength of single lap bonded steel joints bonded with pure epoxy under semi-static load and epoxy bonded with nano-silica. They stated that adding 10% and 20% by weight of nano-silica to the epoxy matrix increased the adhesive strength by 20%.

2.11 Conclusions of Literature Review

Fibre reinforced polymer composites (FRP) are superior to metals in terms of specific strength, hardness, corrosion resistance and formability. However, metals have significant advantages in terms of their high reliability and their ability to be used in almost any ambient conditions, impact resistance, wear and temperature resistance, production costs. Moreover, in practical applications it is almost impossible to make an entire body as a single body, so the combination of metals and composites is inevitable. For this reason, large structures such as ships and planes are made of composite materials and metals called hybrid structures. Composite and

metal hybrid constructions are key technologies for other industries in terms of their high hardness, light weight and reliability. One of the main objectives is to reduce the weight of the vehicles by using light building materials in the aviation and automotive industry and thus to provide fuel consumption. New trends in production, such as light weight, increased performance and functionality, increase the need to use hybrid assemblies and thus to combine unique materials. In recent years, light metals such as aluminium, magnesium and titanium alloys and various fibre reinforced (glass, carbon, kevlar etc.) polymers have been combined for a very strong and light hybrid structure.

Adhesively bonded joints used to combine different types of materials offer significant advantages to designers in terms of low number of parts used, light weight, installation time, stress accumulation, sealing, cost, improved fatigue and corrosion resistance, smoothness and aesthetics.

Epoxy adhesives are adhesives with excellent chemical and corrosion resistance as well as high mechanical and thermal properties. However, such adhesives have poor resistance to low fracture toughness and hence high crack formation due to the cross-linked structures. Nano-particles exhibiting many unique mechanical properties have become one of the most attractive options in recent years to increase the strength of polymeric materials and adhesives.

When we look at the literature, it is seen that Nano-particles are being added to epoxy or polymer adhesives to study how they affect the mechanical properties of Nano-composites or direct bulk adhesives. However, the mechanical connections and the degradation processes of the adhesively bonded joints are very complex. And also many factors such as the type of adhesive, the type of adherent materials, the overlay length and the thickness of the adhesive affect the strength of the connections. Therefore, these effects need to be better understood by using different Nano-particles, different adherents and different adhesives. So, in this study, the effects of adding Nano-particles such as Nano-silica, Nano-clay and multi-walled carbon Nano-tubes (MWCNT) to commercial epoxy adhesive (Araldite 2014) on the shear and impact strength of Al-GFRP single-lap joints are investigated.

CHAPTER 3

EXPERIMENTAL STUDIES

3.1 Introduction

In this chapter, materials and their properties to produce single-lap adhesive bonding joints for experimental studies are explained and how five different experimental tests are carried out.

3.2 Adherent Materials

Adhesively bonded metal and fibre reinforced polimer composite joints are carried out in this thesis. Three types of aluminium plates and glas fibre reinforced polymer GFRP plates as adherents have been used.

3.2.1 Aluminium Plates

Due to fair physical and mechanical properties and high corrosion resistance, aluminium alloys are frequently preferred in aviation and automotive industries. In this study three types of Aluminium alloys (1050, 7075-T6 and 2024-T3) were used as adherents. All plates are 2 mm thickness. 1050 Aluminium (Table 3.1 and 3.2) is a 1000-series aluminium alloy. This alloy is known for its excellent corrosion resistance, high ductility, and highly reflective finish. It has low mechanical strength compared to more significantly alloyed metals. Plates were obtained from the company “Conrad”.

Table 3.1 Chemical composition of aluminium alloy 1050A

Component wt. %	**Fe**	**Si**	**Cu**	**Cr**	**Mn**
	0.5	0.5	3.8-4.9	0.1	0.3-0.9
	Mg	**Zn**	**Zr+Ti**	**Others**	**Al**
	1.2-1.8	0.25	0.15	0.15	Remain

Table 3.2 Mechanical properties of aluminum alloy 1050A

Yield Strength (Mpa)	Tensile Strength (Mpa)	Elongation (%50)	Hardness (Brinell)
340	475	18	120

Aluminium 7075-T6 (Table 3.3 and 3.4) is a high strength material used for highly stressed structural parts such as, aircraft fittings, gears and shafts, regulating valve parts, worm gears, keys, aircraft, aerospace and defence applications. Plates were bought from “Seykoç Aluminum Company”.

Table 3.3 Chemical composition of aluminum alloy 7075-T6

Component wt. %	Fe	Si	Cu	Cr	Mn
	Max . 0.5	Max. 0.4	3.8-4.9	0.18-0.28	Max . 0.3
	Mg	**Zn**	**Zr+Ti**	**The Others**	**Al**
	2.1-2.9	5.1-6.1	0.25	0.15	Remain

Table 3.4 Mechanical properties of aluminum alloy 7075-T6

Yield Strength (Mpa)	Tensile Strength (Mpa)	Elongation (%50)	Hardness (Brinel)
503	572	11	150

The Al 2024-T3 Aluminium alloy (Table 3.5 and 3.6), also known as duralumin, is one of the hardest aluminium alloys with the highest modulus of elasticity and strength. It is widely used in automotive industry, wagon construction, aircraft fuselage and wings, orthopaedic base, rivets and tractor wheels where specific strength (yield strength / density) and specific elasticity module (elasticity modulus/ density) are important. Plates were bought from “Seykoç Aluminum Company”.

Table 3.5 Chemical composition of Aluminum Alloy 2024-T3

Component wt. %	Fe	Si	Cu	Ti	Mn
	0.-0.4	0.-0.25	0-0.05	0-0.05	0.-0.05
	Mg	**Zn**	**The Others**	**Al**	
	0.-0.05	0.-0.07	0-0.03	Remainder	

Table 3.6 Mechanical properties of Aluminum Alloy 2024-T3

Yield Strength (MPa)	Tensile Strength (MPa)	Elongation (%50)	Hardness (Brinel)
85	105-145	12	34

3.2.2 Glass Fibre Reinforced Polymer (GFRP) Plates

Fibre reinforced polymer (FRP) composite materials are widely used in aerospace, civil and structural industries because of several favourable properties such as low density, high specific strength and stiffness. In addition, the fatigue strength to weight ratios as well as fatigue damage tolerances of many composite laminates is excellent. Thus, FRP composites have emerged as a major class of light-weight structural material. In this study, Glass Fibre Reinforced Polymer G10-FR-4 plate with 2 mm thickness was used. G10-FR-4 glass fibre reinforced polymer (see Table 3.7) platters are thermosetting industrial fibreglass composite laminates made of epoxy resin-bonded continuous filament glass fibre material. Initially marketed in the 1950s, this product has high strength, low moisture absorption, excellent electrical properties and chemical resistance. Important properties are shown in Table 3.7. Plates were purchased from company "Kupar Pompa, Küçükparmak Mühendislik San. Tic. Ltd. Şti.".

Table 3.7 Properties of GFRP

Properties	
Density (g/cm^3)	17.101
Buckling Strength (MPa)	357
Tensile Elastic Modulus (MPa)	23752
Pressure Resistance (N/mm^2)	371.2
Notch Impact Strength (Parallel to Lamination) (kJ/m^2)	117.79

3.3 Epoxy Adhesives

Epoxy adhesives contain an epoxy resin and a hardener. Due to the presence of many resins and many different hardeners, they provide flexibility in the formulation. Epoxy adhesives can be used to join most materials. In this study, Carbon Kleber CG4 and Araldite 2014-1 (see Table 3.8), two component, room temperature curing, environmentally sensitive, chemical resistant high viscosity epoxy adhesives, were used as adhesives. These adhesives are particularly suitable for bonding metal to metal, glass fibre and carbon fibre polymers. Their characteristics are given in Table 3.8. The Carbon Kleber CG-49, which is used only for Mode I Test, is bought from company 'Conrad'. Araldite 2014-1 used for Mode II toV Tests was purchased from 'Dost Kimya'.

Table 3.8 Properties of adhesives

Properties	Carbon Kleber CG-49	Araldite 2014-1
Hardener- Epoxy Rate	1/2	1/2
Color	Black	Dark Grey
Curing Time (At room Temp.)	7 days	40 minutes
Viscosity (MPa s)	300	100
Tensile Strength (MPa)	26	19
Shear Modulus (MPa)	5	4

3.4 Nano-Particles

3.4.1 Multi Walled Carbon Nano-Tubes (MWCNT)

Carbon nano-tube, a carbon allotropic material, is a tubular nanometer-scale tube (see Figure 3.1) with excellent electrical and optical properties. Multi-walled carbon nano-tubes are a collection of tubes that are nested in ever-increasing diameters and have diverse potential applications in different areas such as medicine, mechanics, electricity-electronics, chemicals, energy. The MWCNTs used in this thesis are functionalised as multi walled carbon nano-tubes (Purity > 96%, Outside Diameter: 8-18 nm) and are purchased from the company 'Nanografen'. The properties are shown in Table 3.9.

Table 3.9 Properties of MWCNT

Properties	
Purity (%)	>96
-COOH Content (%)	2.2
Out Diameter (nm)	8-18
In Diameter (nm)	5-10
Length (μm)	10-35
Surface Area (m^2/g)	>210
Color	Black
Ash (wt.%)	1.5
Electrical Conductivity (S/cm)	98
Density (Tap) (g/cm^3)	0.3
Density (True) (g/cm^3)	2.4

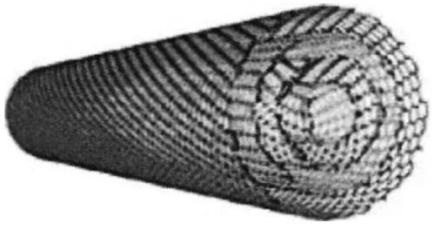

Figure 3.1 Idealized multi walled CNT [61]

3.4.2 Nano-Silica particles

Nano-silica particles (purchased from the 'Grafen Kimya Endustry') are used in 99.5% purity, 15 nm dimensions. Silica (SiO_2) is widely used as filler in polymer and rubber industry. Silica materials have water and thermal stability (up to 1500 °C), good mechanical strength and toxic as well as excellent physical and chemical properties. Their properties are shown in Table 3.10.

Table 3.10 Properties of nano-silica

Properties	
Purity (%)	99.5
Bulk Density (gr/cm^3)	0.05
Average particle size (nm)	15-35
Specific surface area (m^2/g)	300

3.4.3 Nano-Clay Particles

The nano-clay particles used are montmorillonite nano-clay particles at 1-10nm sizes with dimethyl dialkyl amine (properties are shown in Table 3.11). Montmorillonite (MMT) is hydrated alumina-silica clay composed of a central alumina octahedral layer and two tetrahedral layers.

The Na+ and Ca_2+ ions present at the interfaces become lipophilic by the ion exchange reactions with organic cations, such as alkyl ammonium ions, whereby the clay is dispersed in the organic polymer phase.

Table 3.11 Properties of nano-clay

Properties	
Loss in Drying (%)	**<**3
Mass Density (kg/m^3)	200-500
Lateral Width (μm)	0.5-2
Thickness (nm)	1-10

3.5 Experimental Tests

In this study, five tests were carried out from Mode I to Mode V. In all test modes shear strength of adhesively bonded joints were investigated. In last two group of tests (Mode IV and V) Charpy impact test were applied to determine the impact energy for nano-silica and nano-Clay reinforced adhesively bonded joints.

3.5.1 Shear Test

Single lap joint is a mostly used method in adhesively bonding joint and has been the subject of significant research in the last decades. Due to simplicity and efficiency, single lap joints (Figure 3.2) are often used to determine the mechanical properties of adhesively bonded joints. So, for the aim of this thesis, the single lap joints configuration was selected to bind Al- GFRP plates. Lap shear tests are quick and economical way to assess shear strength.

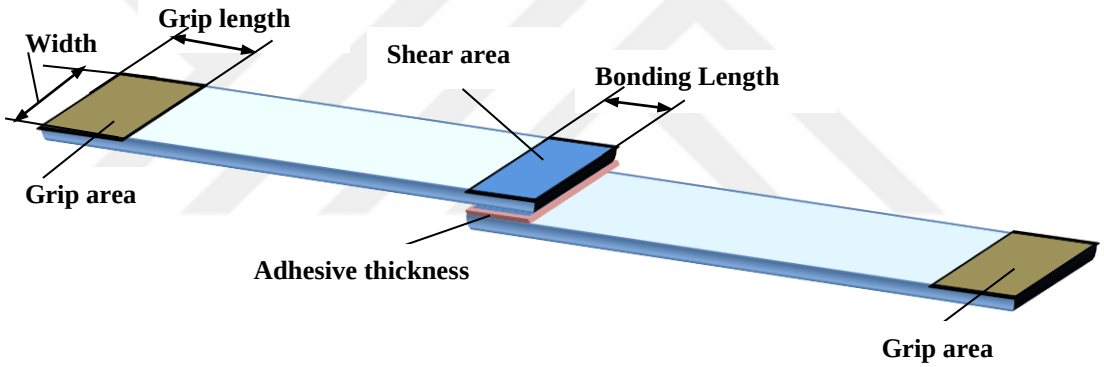

Figure 3.2 Single lap joint configuration

A universal testing machine Shimadzu AG-X (Figure 3.3) with a capacity of 300 kN was used to perform shear strength of single lap joints. The lower head is fixed while the upper head moves with selected constant speed. To measure the direct shear strength of the parts subjected to the tensile test, 25 mm × 25 mm pplates of 2 mm thickness were affixed to the ends (grip area) as shown in Figure 3.4. Samples were pulled at extension rates of 1.0 mm/min until failure, based on ASTM D 3039 standards. Force values and corresponded displacements were recorded through the control unit of test machine. These values were used to evaluate shear strength of worked samples.

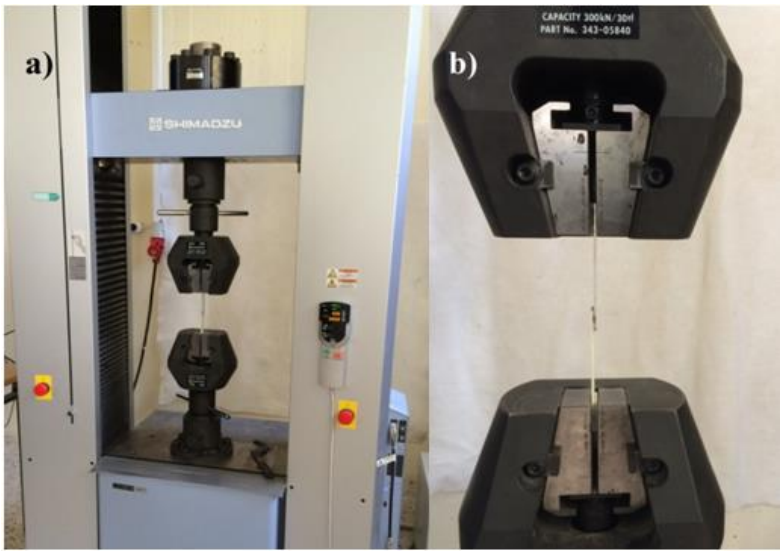

Figure 3.3 (a)- Shimadzu AG-X tensile testing machine, (b)- Test illustration

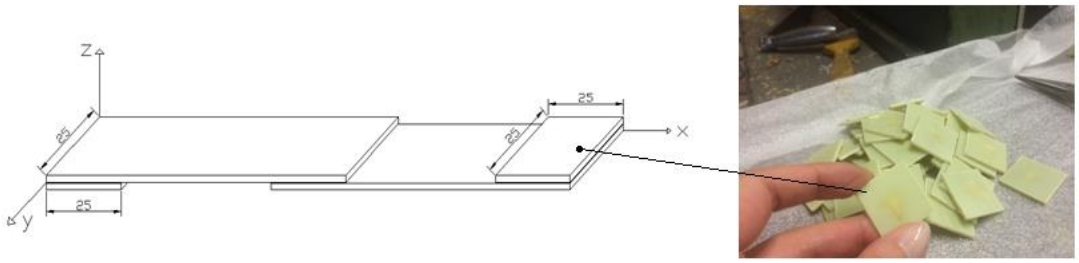

Figure 3.4 25mm×25mm GFRP for Samples' Ends

After applying the tensile tests of the samples, the shear stress with respect to the maximum tensile strength was calculated by Equation 3.1.

$$\tau = \frac{F}{w*b} \qquad (3.1)$$

Where;

- F is the fracture force (N)
- *w* is the bond width (mm), and
- *b* is the overlap length (mm)
- τ is the shear strees (MPa)

3.5.2 Charpy Impact Test

The charpy impact test was used as a fast and cost-effective comparison tool to investigate the impact energy of Al-GFRP adhesively bonded joints. The Charpy impact test is a dynamic three-point bending test of a notched beam. The Kögel 3/70

Charpy impact tester was used in this study; consisting of an anvil supported freely by the sample and a pendulum with mass attached to a rotating arm fixed in the body of the machine (Figure 3.5).

The Charpy impact test is carried out in four general steps. These;

- Calibrating the measurement scale to add the friction losses to the account,
- Placing the samples horizontally in anvils,
- Giving the impact load to the sample by the pendulum and
- Measurement of the breaking energy with a constant gauge.

The breakdown energy is determined based on the difference between the initial height of the pendulum (h_a) before release and the potential energy of the maximum height (h_b) of the post-impact pendulum (Figure 3.5-a).

$$U=m_x g_x (h_a-h_b) \qquad (3.2)$$

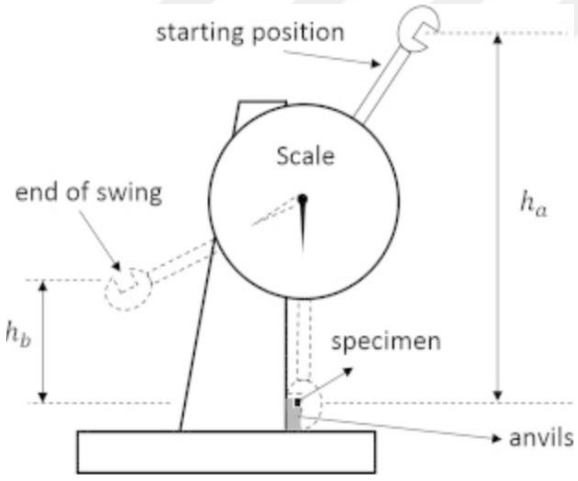

(a)

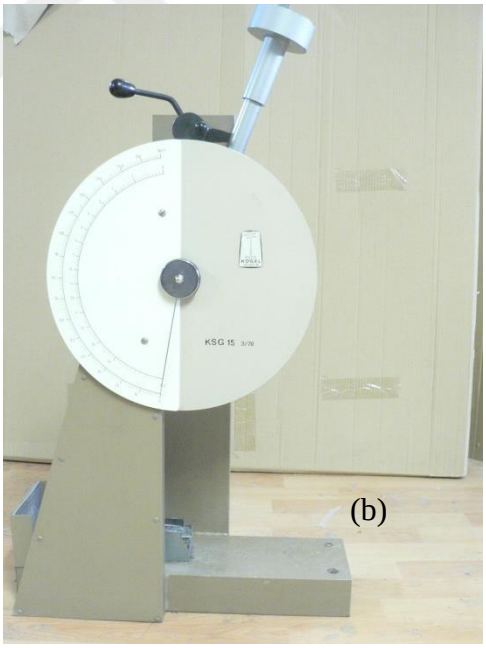

(b)

Figure 3.5 Charpy impact test illustration (a) Kogel 3/70 charpy impact device (b)

3.5.3 Specimens Preparation

Firstly, Al and GFRP plates were cut by guillotine in dimensions of 100mm×25mm for tensile test and 55mm×10mm for Charpy impact test (Figure 3.6 and 3.7).

Then, the sample surfaces were abraded with Nikon 100-C silicon carbide abrasive paper. Surface preparation of the substrates which have to be bonded is a very

important step in the sample preparation as it directly affects the bond strength of the adhesive and indirectly affects the failure mode. By preparing a bonding surface to required specifications the bond strength can be at its full potential and hence resulting in a longer structural life. The major role of surface preparation is to remove macro and micro impurities from the surface of the adherent in order to, increase the surface area of the adherent and thus improving the surface roughness. To remove wastes such as oil, dirt and dust on the samples, they were cleaned with pure acetone and allowed to stand until the acetone had completely evaporated.

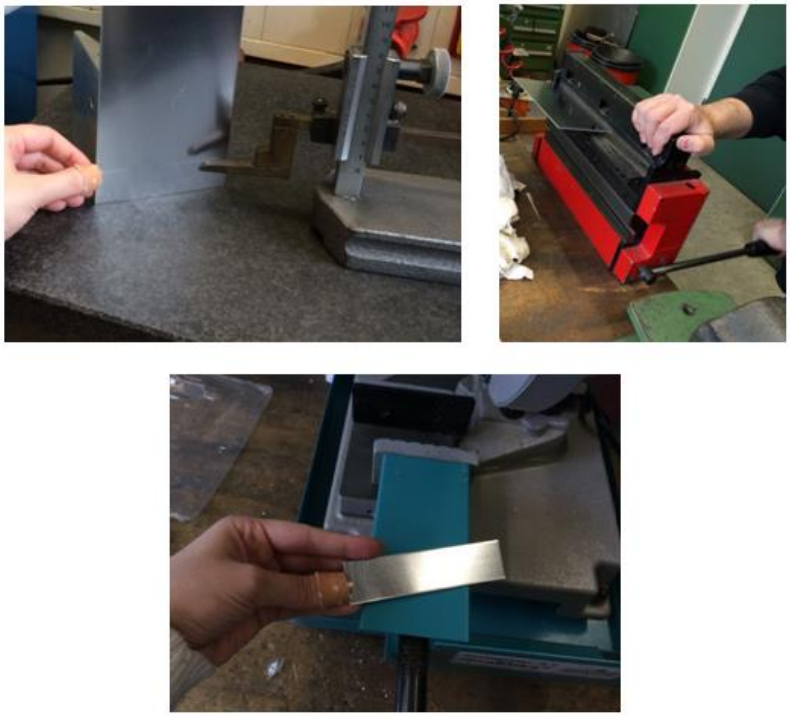

Figure 3.6 Cutting of adherents' plates by guillotine

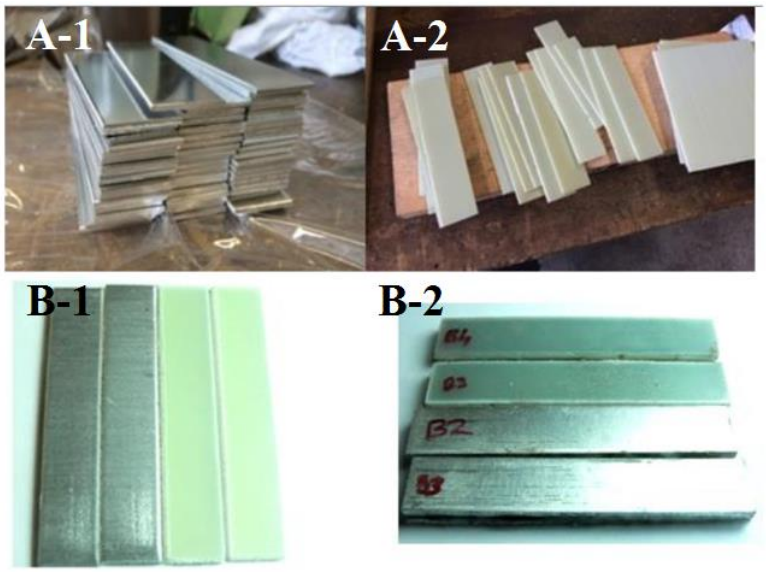

Figure 3.7 Aluminum and glass fibre composite samples: (A1 & A2)- Samples for tensile test, (B1&B2)- Samples for Charpy impact test

3.6 Mode I Tests

Mode I test are conducted to select suitable commercial adhesive and to find suitable input parameters that effect bonding quality such as overlap area, surface quality, spew formation, etc. Two types commercial epoxy adhesive, name by Carbon Kleber CG-49 and Araldite 2014-1, were compared (Figure 3.8) and four overlap lengths were examined.

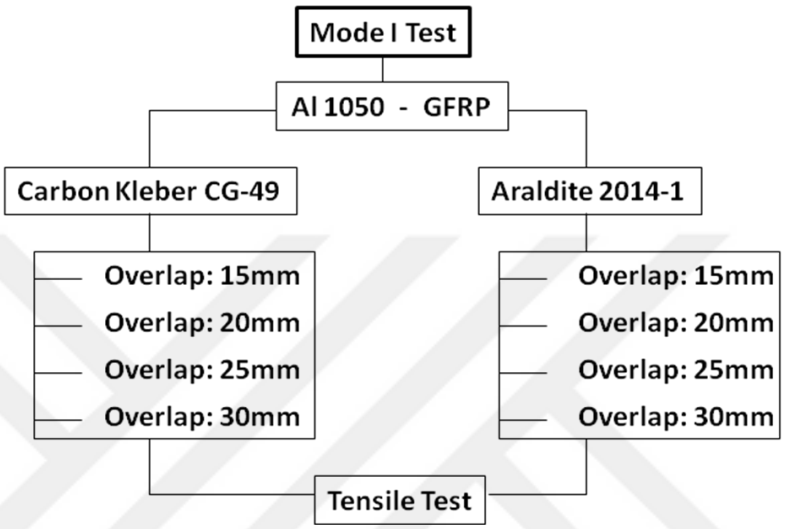

Figure 3.8 The roadmap of Mode I Test

Specimens were cut according to the measurements determined from GFRP and aluminium 1050 plates, the surfaces of the specimens were sanded to make the roughness suitable, and the surfaces were cleaned, glued and the bonded specimens were subjected to tensile test.

3.6.1 Adhesive Preparation

For this Mode, Araldite 2014-1 and Carbon Kleber CG-49 adhesives were used. As shown in Figure 3.9, these two adhesives were consisting of two-phase state which are epoxy resin and hardener.

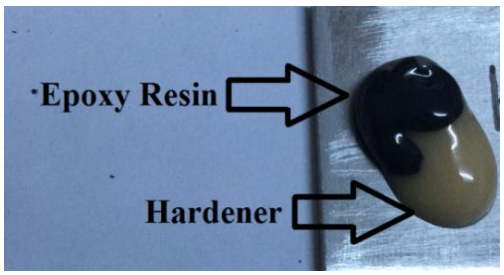

Figure 3.9 Illustration of epoxy and hardener

Before the application, adhesive's hardener and epoxy resin are prepared to be mixed with ½ ratio of the mixture by hand for 10-15 seconds.

3.6.2 Sample Preparation

It is known that the adherent surface areas should not be very bright for adhesive joints, and the wedge effect of roughness is left out in very bright places. This information is shaded with first 100, then 400 grid sandpaper after cutting with guillotine for lengths of different overlaps (15, 20, 25, 30 mm) in the region where the adhesive (b= overlap length) applied (see Figure 3.10). The surfaces of the samples were cleaned with the help of pure acetone (Figure 3.11).

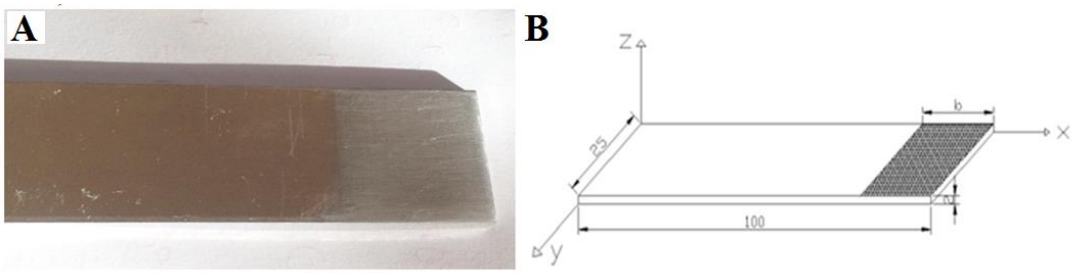

Figure 3.10 (A)- Sanded area on aluminum plate, (B)- Plate size (100mm×25mm×2mm)

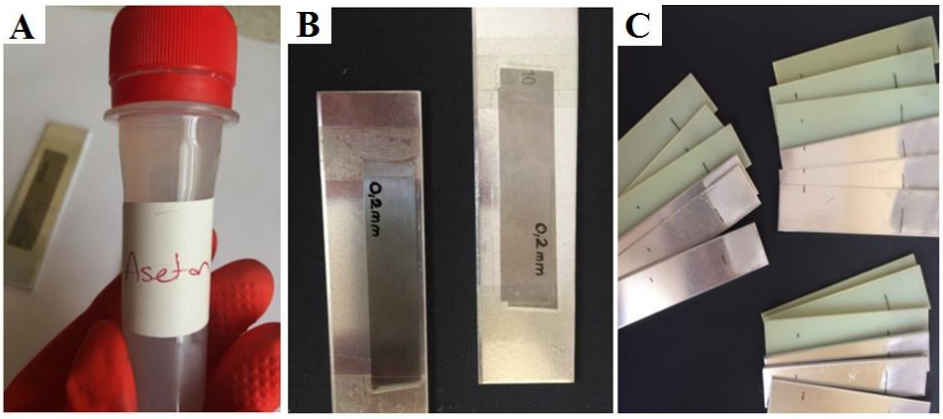

Figure 3.11 (A) Acetone used for surface cleaning, (B) 0.2mm Plate used to adjust the adhesive thickness, (C) Measured and ready to use samples

3.6.3 Application of Adhesive

0.2 mm thickness scale sheets were used to apply the adhesive (Figure 3.12 and 3.13) by doctor blading method. Carbon Kleber CG-49 applied samples were completed at room temperature (23°C) for seven days of drying time. Likewise, Araldite 2014-1 applied specimens were completed at room temperature for one day of drying time.

Extra adherents were supported to the samples after application till the end of curing time as shown in Figure 3.14.

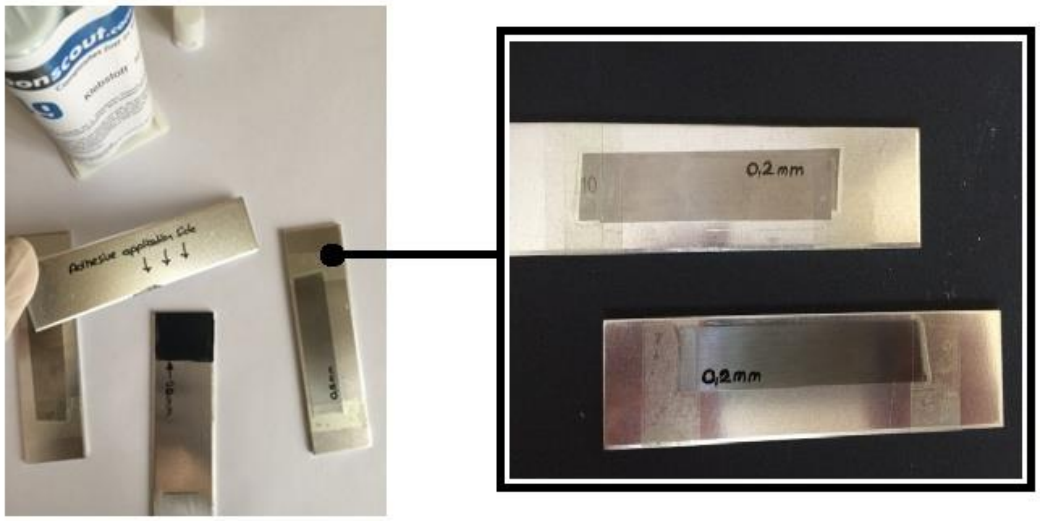

Figure 3.12 0.2 mm scale sheets on 2 mm samples

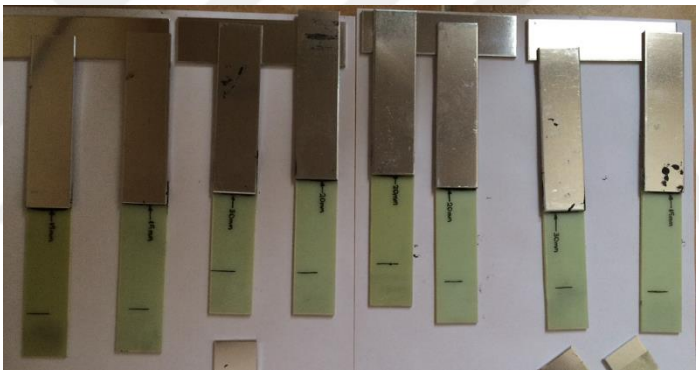

Figure 3.13 Samples' curing illustration

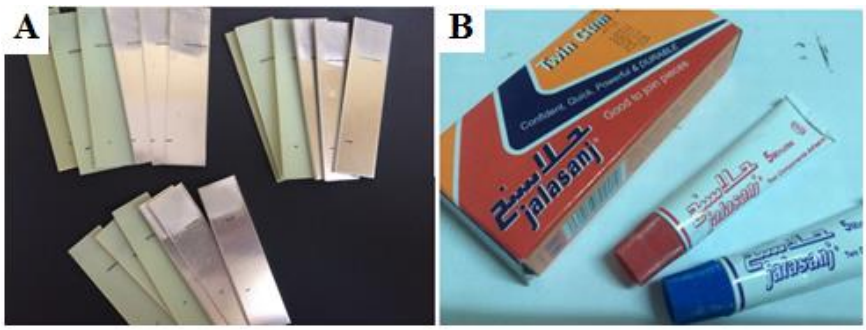

Figure 3.14 (A)- Marking on samples, (B)- Two phase glue for end of samples

The samples were subjected to axial tensile testing with a universal testing machine Shimadzu AG-X (Figure 3.15) with a capacity of 300 kN in accordance with ASTM D 3039 standards.

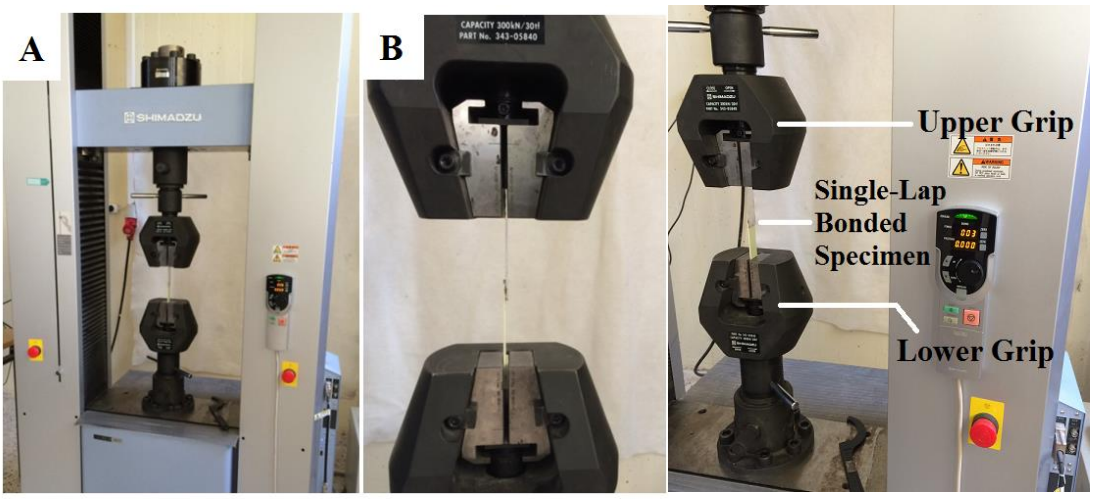

Figure 3.15 (A)- Shimadzu AG-X tensile testing machine, (B)- Test illustration

Samples are designated by adhesive name and overlaps. Carbon Kleber CG-49 and Araldite 2014-1 (Figure 3.16) adhesives were prepared as a total of 24 specimens in three pieces according to the overlap lengths of 15, 20, 25, 30 mm (Figure 3.17). The coding of the samples is given in Table 3.12.

Figure 3.16 Sample illustration with its code

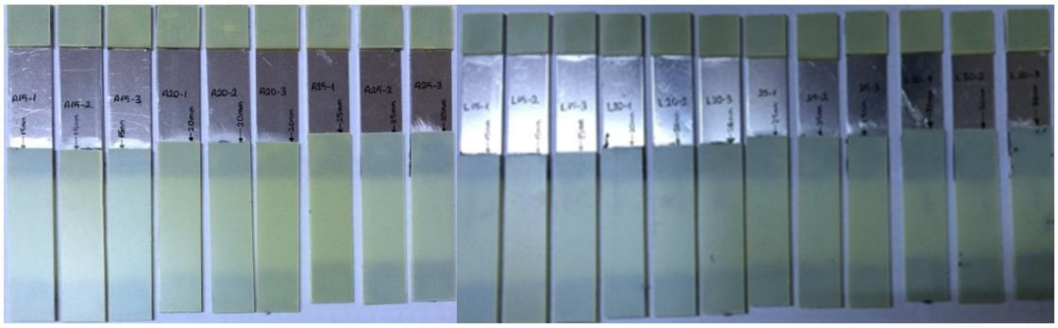

Figure 3.17 Test samples with different overlaps

Table 3.12 The coding of the samples

Sample Code	Overlap Length (mm)	Adhesive Type
C15	15	Carbon Kleber CG-49
C20	20	Carbon Kleber CG-49
C25	25	Carbon Kleber CG-49
C30	30	Carbon Kleber CG-49
A15	15	Araldite 2014-1
A20	20	Araldite 2014-1
A25	25	Araldite 2014-1
A30	30	Araldite 2014-1

After the finish of curing time, spew formation on edges was observed (Figure 3.18). It was normal when considering the samples' weight and the curing condition with supporting adherent. It was cut out with a knife.

The samples were tested at a feed rate of 1mm/min. Experiments were performed at room temperature (23°C) and the results were recorded.

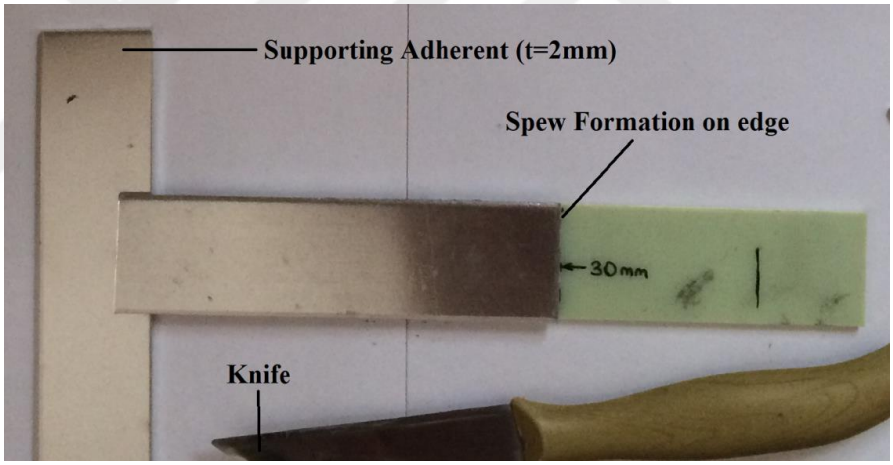

Figure 3.18 Spew formation illustration on sample

3.7 Mode II Tests

According to the test results of Mode I tests, Araldite 2014-1 was selected as an adhesive and overlap length was taken as 25 mm for Mode II test, so then the roadmap (Figure 3.19) is figured out for this adhesive according to the percentage by weight of nano-particles. In this test, one of the adherents was aluminium alloy 7075-T6 plates, the surfaces of the specimens were sanded to make the roughness suitable and the surfaces were cleaned (Figure 3.20). In Mode I tests, due to according to measurement of adhesive thickness was differ ±0.01 mm from desired thickness.

Although this reduction is quite small, an adhesively bonding pattern was designed and manufactured (see Figure 3.21) so that negative situations that might occur due to this bonding condition would not affect the test results in Mode II.

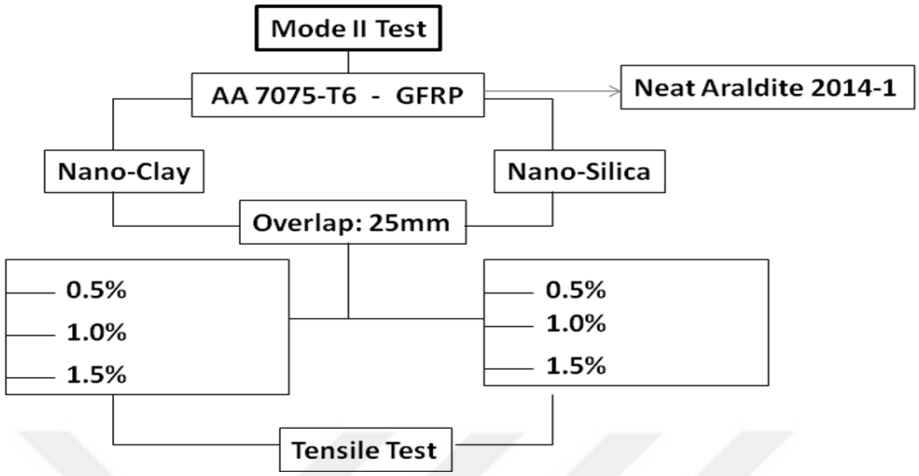

Figure 3.19 The roadmap of Mode II Test

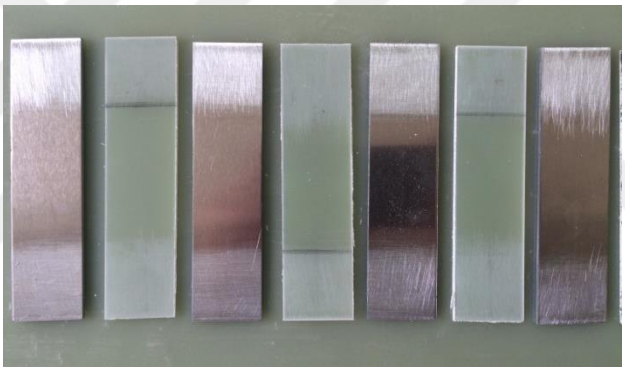

Figure 3.20 Surface roughnesses of adherents illustration

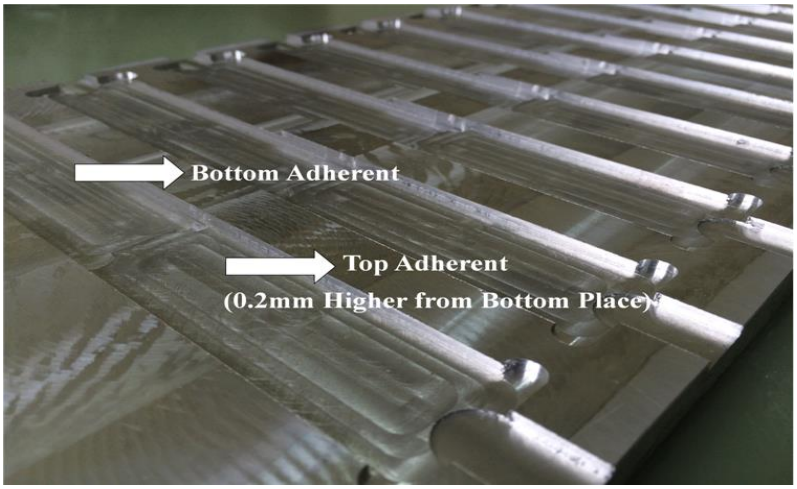

Figure 3.21 Test pattern

In this mode, adhesives were prepared with nano-silica and nano-clay particles by weight of 0.5%, 1% of 1.5%. Three samples were fabricated for each percentage. To mix nano-particles and Araldite 2014 firstly, the glasses were cleaned (Figure 3.22-A). Then, Adhesive's hardener and epoxy resin were prepared with ½ ratio of the mixture in a clean glass. And then, according to adhesive weight and percentage rate, nano-particles added. Precision scale (Figure 3.22-B) was used to adjust the weights.

Figure 3.22 (A) Cleaning of glasses by soap and water, (B) Precision scale illustration

After that, acetone was added in the same weight with the adhesive to dilute the mixture and mix the nano-particles better. Finally, nano-particles were added. They were mixed for 50-60 minutes by hand till evaporation of the acetone. Such evaporation also was checked by a scale. GFRP plates were placed on manufactured pattern and the prepared adhesive mixture was applied to the surface of the samples with a stick. Then, coding of the samples was employed as seen at Table 3.13. The adhesive which is 0.2 mm thick was applied to the related section of the plate. After that, aluminium plates were placed (Figure 3.23) then the curing time started.

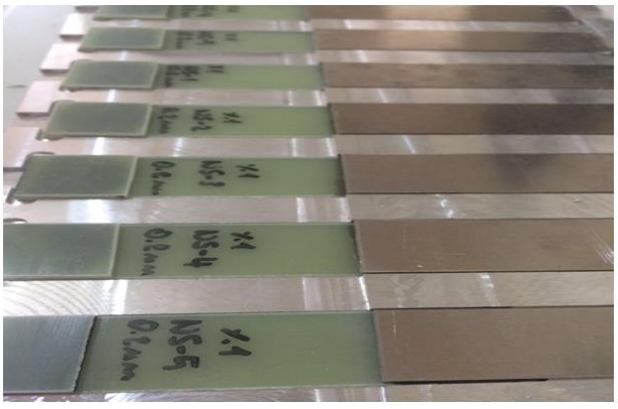

Figure 3.23 Illustration of the samples on pattern

Table 3.13 The coding of the samples

ADHESIVE	Adhesive Weight (gr)	Nano-Particle	Nano-Particles Weight (gr)	Specimen Code
ARALDITE 2014-1	10	CLAY	0.05	%0.5 NC-1
				%0.5 NC-2
				%0.5 NC-3
				%0.5 NC-4
				%0. 5 NC-5
ARALDITE 2014-1	10	CLAY	0.1	%1 NC-1
				%1 NC-2
				%1 NC-3
				%1 NC-4
				%1 NC-5
ARALDITE 2014-1	10	CLAY	0.15	%1.5 NC-1
				%1.5 NC-2
				%1.5 NC-3
				%1.5 NC-4
				%1.5 NC-5
ARALDITE 2014-1	10	SILICA	0.05	%0.5 NS-1
				%0.5 NS-2
				%0.5 NS-3
				%0.5 NS-4
				%0.5 NS-5
ARALDITE 2014-1	10	SILICA	0.1	%1 NS-1
				%1 NS-2
				%1 NS-3
				%1 NS-4
				%1 NS-5
ARALDITE 2014-1	10	SILICA	0.15	%1.5 NS-1
				%1.5 NS-2
				%1.5 NS-3
				%1.5 NS-4
				%1.5 NS-5

Samples were cured at room temperature (23°C) for two days. After that, the samples were removed from the pattern. No spew formation was observed as shown in Figure 3.24. The thickness was checked and it was made sure that there was a 0.2 mm adhesive thickness. At the end, adhesively bonded samples were subjected to axial tensile testing.

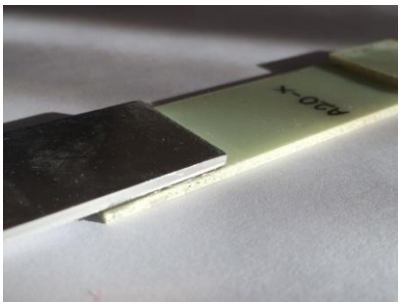

Figure 3.24 Samples are ready to use without any spew formation

3.8 Mode III Tests

Experience gained in Mode II tests showed that the uniform distribution of nano-particles in the adhesive is a very important parameter that affects the test results. The roadmap (Figure 3.25) is used for this adhesive according to the percentage by weight of nano-particles.

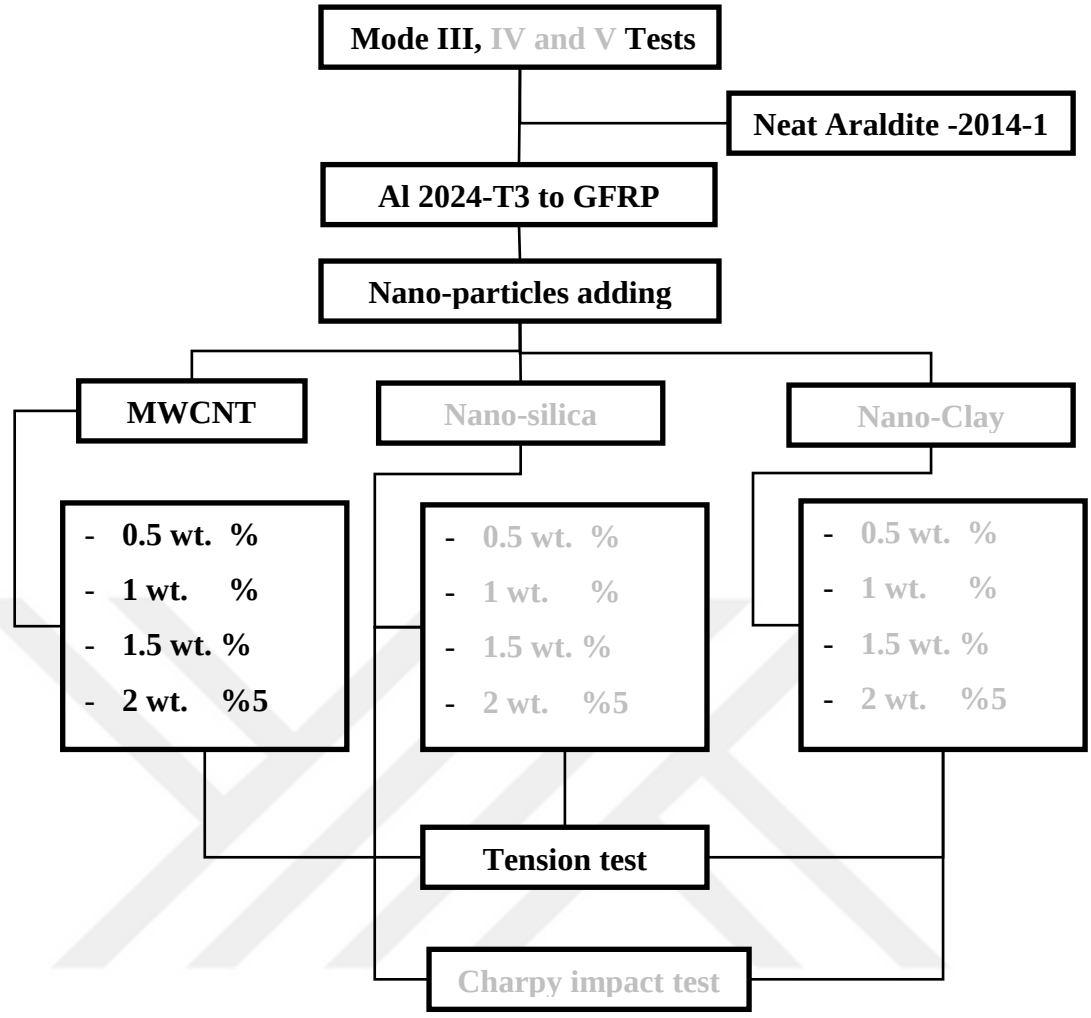

Figure 3.25 The roadmap of the Mode III Test with MWCNT

3.8.1 Adhesive Preparation

In the preparation of MWCNT additive adhesive, Araldite 2014-1 epoxy adhesive and hardener (½ ratio) were added to the desired amount of 0.01gr precision scale in a clean beaker glass (Figure 3.26-A). Nano-particles were added in the weight ratio of 0.5%, 1%, 1.5% and 2%, respectively. The highly viscous adhesive was mixed with a 1:1 ratio of Merck 100014 brand acetone (C_3H_6O) in 99% purity. It was mixed with a light load homogenizer at 22,000 rpm for 30 minutes (Figure 3.26-B). The acetone was left under the curing temperature until it completely disappeared from the mixture, and it was controlled on the sensitive scale.

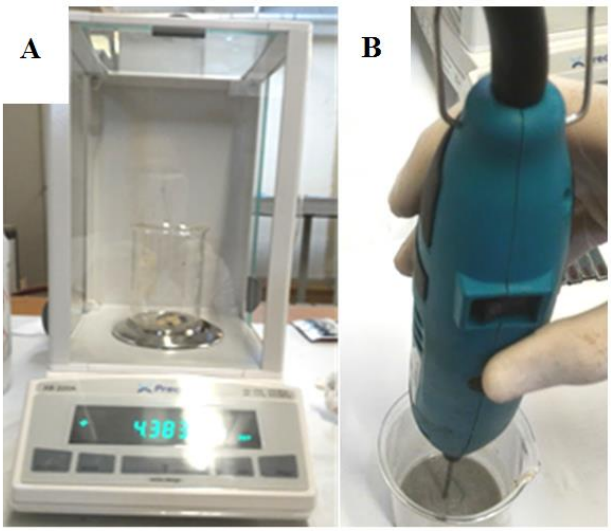

Figure 3.26 (A) Presicion scale, (B) Homogenizer

As in case of Mode II tests, specimens were cut to size; their surfaces were prepared and cleaned. After the sample preparation, the adhesive prepared for the designated areas in the samples was applied at a thickness of 0.2 mm. Curing time is also started after the codes are exported to the samples (Table 3.14).

Table 3.14 The coding of samples of Mode III Test

Adhesive	Nano-Particle	Specimen Code
Araldite 2014-1	0.25 wt. % MWCNT	**C0-1**
Araldite 2014-1	0.25 wt. % MWCNT	**C0-2**
Araldite 2014-1	0.25 wt. % MWCNT	**C0-3**
Araldite 2014-1	0.25 wt. % MWCNT	**C0-4**
Araldite 2014-1	0.25 wt. % MWCNT	**C0-5**
Araldite 2014-1	0.50 wt. % MWCNT	**C1-1**
Araldite 2014-1	0.50 wt. % MWCNT	**C1-2**
Araldite 2014-1	0.50 wt. % MWCNT	**C1-3**
Araldite 2014-1	0.50 wt. % MWCNT	**C1-4**
Araldite 2014-1	0.50 wt. % MWCNT	**C1-5**
Araldite 2014-1	1.00 wt. % MWCNT	**C2-1**
Araldite 2014-1	1.00 wt. % MWCNT	**C2-2**
Araldite 2014-1	1.00 wt. % MWCNT	**C2-3**
Araldite 2014-1	1.00 wt. % MWCNT	**C2-4**
Araldite 2014-1	1.00 wt. % MWCNT	**C2-5**
Araldite 2014-1	2.00 wt. % MWCNT	**C3-1**
Araldite 2014-1	2.00 wt. % MWCNT	**C3-2**
Araldite 2014-1	2.00 wt. % MWCNT	**C3-3**
Araldite 2014-1	2.00 wt. % MWCNT	**C3-4**
Araldite 2014-1	2.00 wt. % MWCNT	**C3-5**
Araldite 2014-1	1.50 wt. % MWCNT	**C4-1**

Araldite 2014-1	1.50 wt. % MWCNT	**C4-2**
Araldite 2014-1	1.50 wt. % MWCNT	**C4-3**
Araldite 2014-1	1.50 wt. % MWCNT	**C4-4**
Araldite 2014-1	1.50 wt. % MWCNT	**C4-5**
Araldite 2014-1	0.75 wt. % MWCNT	**C5-1**
Araldite 2014-1	0.75 wt. % MWCNT	**C5-2**
Araldite 2014-1	0.75 wt. % MWCNT	**C5-3**
Araldite 2014-1	0.75 wt. % MWCNT	**C5-4**
Araldite 2014-1	0.75 wt. % MWCNT	**C5-5**

The samples were kept in the mold for 5 days at room temperature (23°C). Subsequently, it has been verified that the thickness of the adhesive is 0.2 mm with the help of a calliper.

3.8.2 Tests

The tensile test was applied to these samples. The test procedure is the same as in the Mode I and Mode II Test.

3.9 Mode IV Tests

The theoretical and practical gains have achieved in Mode I and II have been finalized for Mode III tests. In the desired direction, the results of Mode III were quite satisfactory. For instance, the use of the sample preparation mould and the use of a homogenizer significantly increased adhesive results in order to achieve the required dispersion. Therefore, this test Mode was also followed by the Mode III test. In addition to this mode, the Charpy impact test was added to see the effect of nano-particles adding on impact behaviour of bonded joints. So, both tensile and impact tests are done in mode IV. The roadmap of Mode IV test prepared as in Figure 3.27.

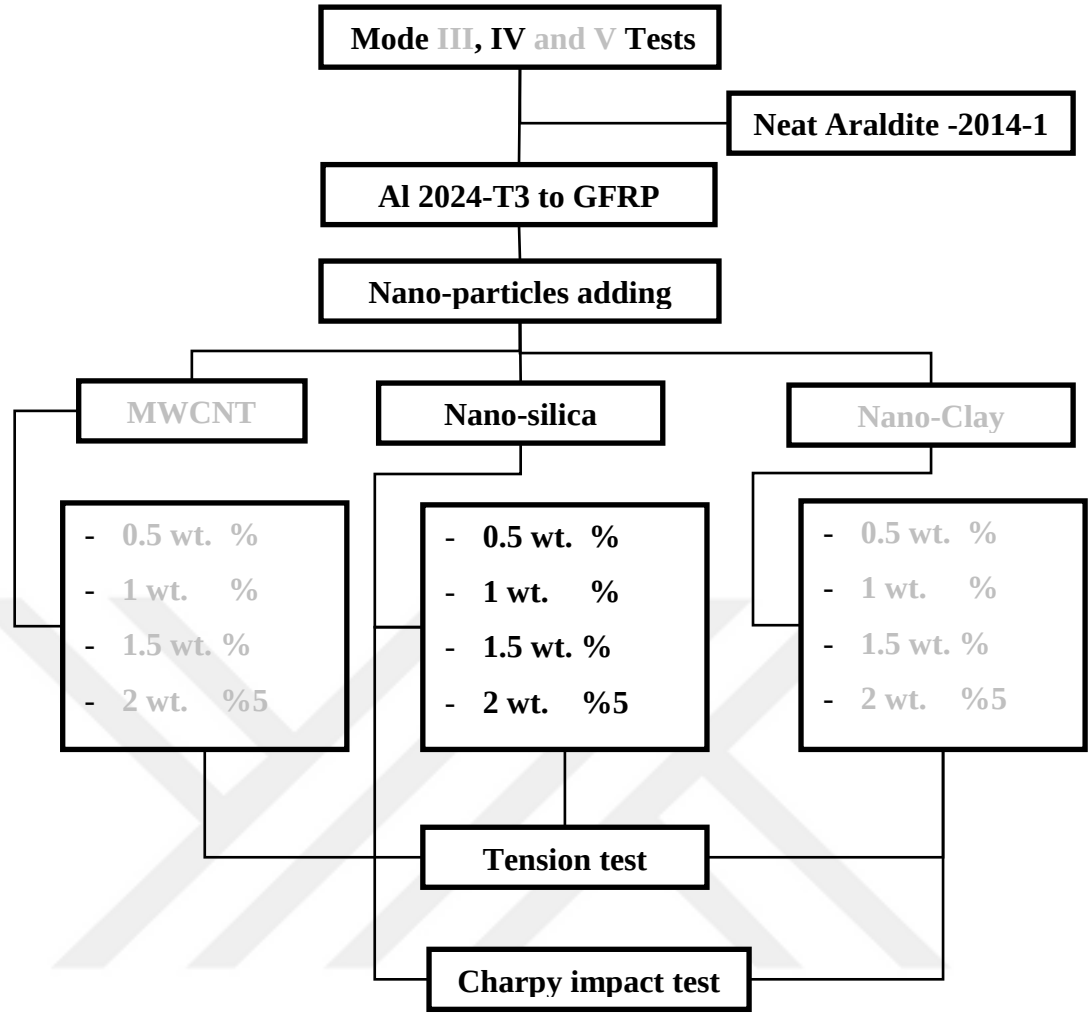

Figure 3.27 The roadmap of the Mode III Test with MWCNT

3.9.1 Adhesive Preparation

As seen in Figure 3.27, the procedure was continued with Araldite 2014-1. Nano-silica particles were added into this adhesive in proportions of by weight 0.5%, 1%, 1.5%, and 2%, respectively, and 4 different mixtures were formed. In addition, a mixture of epoxy and hardener of neat Araldite 2014-1 in a separate glass cup was also prepared to compare the results. The codes for samples are given as in Table 3.15. The curing time and conditions were the same with those in Mode III.

Table 3.15 Codes of Mode IV test's samples

Adhesive	Nano-Particle	Specimen Code
Araldite 2014-1	0.5 wt. % Silica	A1-1
Araldite 2014-1	0.5 wt. % Silica	A1-2
Araldite 2014-1	0.5 wt. % Silica	A1-3
Araldite 2014-1	0.5 wt. % Silica	A1-4
Araldite 2014-1	0.5 wt. % Sılıca	A1-5
Araldite 2014-1	1.0 wt. % Silica	A2-1
Araldite 2014-1	1.0 wt. % Silica	A2-2
Araldite 2014-1	1.0 wt. % Silica	A2-3
Araldite 2014-1	1.0 wt. % Silica	A2-4
Araldite 2014-1	1.0 wt. % Silica	A2-5
Araldite 2014-1	1.5 wt. % Silica	A3-1
Araldite 2014-1	1.5 wt. % Silica	A3-2
Araldite 2014-1	1.5 wt. % Silica	A3-3
Araldite 2014-1	1.5 wt. % Silica	A3-4
Araldite 2014-1	1.5 wt. % Silica	A3-5
Araldite 2014-1	2.0 wt. % Silica	A4-1
Araldite 2014-1	2.0 wt. % Silica	A4-2
Araldite 2014-1	2.0 wt. % Silica	A4-3
Araldite 2014-1	2.0 wt. % Silica	A4-4
Araldite 2014-1	2.0 wt. % Silica	A4-5

3.9.2 Tests

In this mode tensile test and Charpy impact test was applied to these samples. The tensile test procedure was the same as in Mode I, II and III tests. The adhesive was prepared in the same manner for the impact tests. After being controlled on the sensitive scale, the adhesive was applied to the specimens in 55×10 mm dimensions (Figure 3.28).

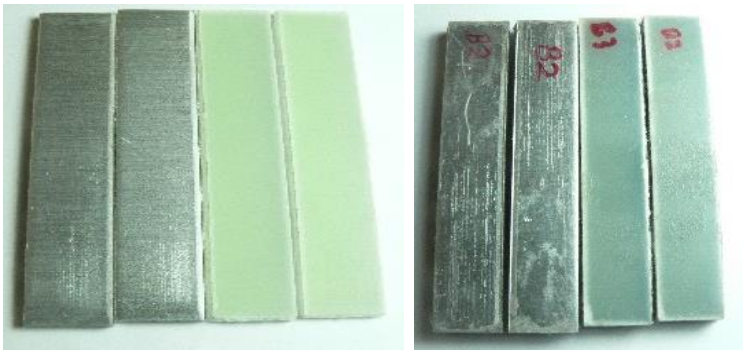

Figure 3.28 Preperation of samples for impact test

For the thickness of the adhesive to be 0.2 mm, a mould with a height of 4.2 mm is prepared. The bonded samples were stored in the mould for 1 day and then 4 days out of the mold for curing. All samples thickness was measured with calliper (Figure 3.29).

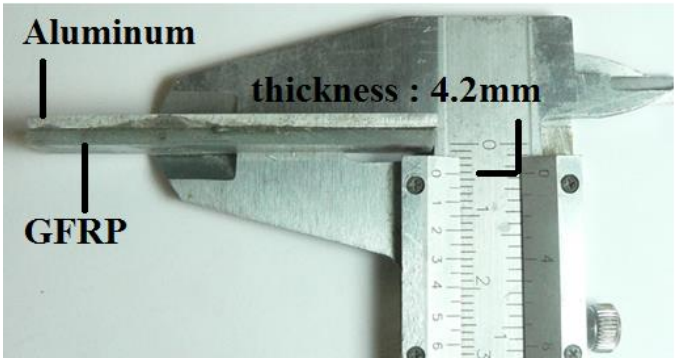

Figure 3.29 Thickness control of bonded samples

In Charpy impact test, 5 different combinations were made, namely 0.5%, 1%, 1.5% and 2% nano-silica added specimens combined with additive-free adhesive and ten specimens were prepared for each type. Experiments were carried out on five of the prepared specimens in the direction of facing aluminium (Figure 3.30 -b) and in the other five in the direction of facing glass fibre polymer (Figure 3.30-c). All tests were conducted at room temperature and standard humidity.

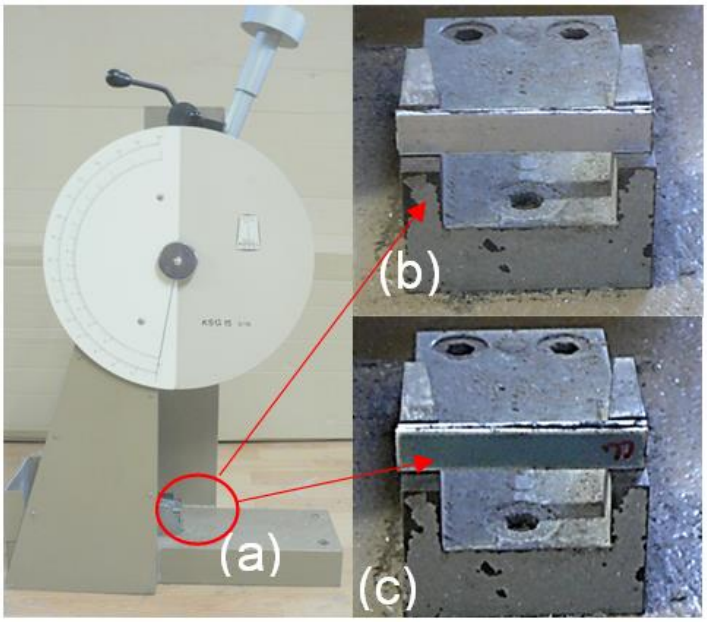

Figure 3.30 (A) The Kogel 3/70 charpy impact device, (B) Aluminum sample (C) and GFRP orientation

3.10 Mode V Tests

The methods used in this section are the same with the test Mode IV however nano-clay is used as the nano-particle. Nano-clay particles were added into Araldite 2014 adhesive in proportions of by weight 0.5%, 1%, 1.5%, and 2%, respectively, and 4 different mixtures were formed. The roadmap of the Mode V test created with the same criteria with Mode IV (Figure 3.31). Tensile test samples are coded as in Table 3.16. In this mode charpy impact test was also applied to 55x10 mm samples as in Mode IV test.

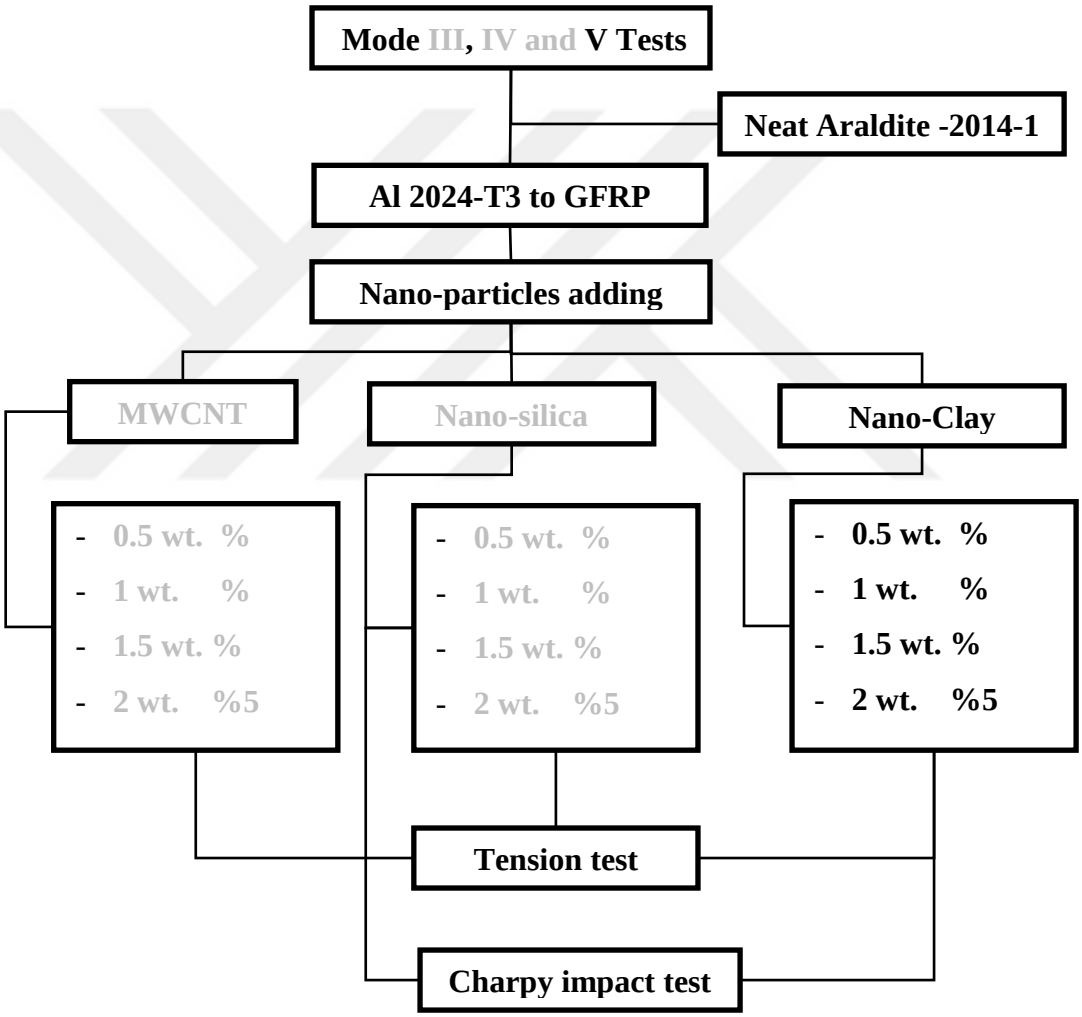

Figure 3.31 The roadmap of the Mode III Test with MWCNT

Table 3.16 Codes of Mode V Test's Samples

Adhesive	Nano-Particle	Specimen Code
Araldite 2014-1	0.5wt. % CLAY	B1-1
Araldite 2014-1	0.5wt. % CLAY	B1-2
Araldite 2014-1	0.5wt. % CLAY	B1-3
Araldite 2014-1	0.5wt. % CLAY	B1-4
Araldite 2014-1	0.5wt. % CLAY	B1-5
Araldite 2014-1	1wt. % CLAY	B2-1
Araldite 2014-1	1wt. % CLAY	B2-2
Araldite 2014-1	1wt. % CLAY	B2-3
Araldite 2014-1	1wt. % CLAY	B2-4
Araldite 2014-1	1wt. % CLAY	B2-5
Araldite 2014-1	1.5wt. % CLAY	B3-1
Araldite 2014-1	1.5wt. % CLAY	B3-2
Araldite 2014-1	1.5wt. % CLAY	B3-3
Araldite 2014-1	1.5wt. % CLAY	B3-4
Araldite 2014-1	1.5wt. % CLAY	B3-5
Araldite 2014-1	2wt. % CLAY	B4-1
Araldite 2014-1	2wt. % CLAY	B4-2
Araldite 2014-1	2wt. % CLAY	B4-3
Araldite 2014-1	2wt. % CLAY	B4-4
Araldite 2014-1	2wt. % CLAY	B4-5

CHAPTER 4

RESULTS AND DISCUSSIONS

In previous chapter, materials and methods used in experimental works were briefly explained and classified. This chapter shows the results of all tension and impact tests for all test modes and also obtained results are discussed.

4.1 Mode I Test Results

Mode I tests were the preliminary experiments. In this mode, the effects of input parameters (i.e. adhesive's types, overlap lengths) on tensile load and shear strength of single lap joints were examined.

Maximum mean tensile load was observed as 3075.17 N with 15 mm overlap length (Table 4.1) with Araldite 2014-1 adhesive used samples. It was also observed that when the overlap length increases, the tensile load decreases by a ratio of 6%, 9% and 23% respectively (Figure 4.1). Maximum shear strength was calculated as 8.2 MPa for Araldite 2014 adhesive type when overlap length was 15 mm (Table 4.1).

Test results of samples with Carbon Kleber CG-49 adhesive showed that when the overlap length increases, the tensile load gradually increases. The maximum tensile load according to the average tensile load values was observed at C30 (30 mm overhang length) series as 5762.34 N.

Comparing the maximum tensile loads of two different adhesives, the maximum load in the C30 series (5672.34 N) was 87% higher than that A15 series (3075.17 N) (Table 4.1). When the shear strength values were compared, the maximum shear strength at C15 (10.8 MPa) was 32% higher than that at A15 (8.2 MPa) (Figure 4.2).

Grant et al. [16] experimentally investigated the effect of the bonding area on the bond strength. They concluded that when the bonding area increased, the shear strength decreased similarly as seen in Figure 4.2 and 4.3. Accordingly, Figure 4.2 maximum shear strength values were obtained in samples A15 and C15.

Table 4.1 Results of Mode I Tests

Adhesive type	Overlap length (mm)	Specimen code	Max. Tensile Load (N)	Shear strength (MPa)	Max. Deformation (mm)
Araldite 2014-1	15	A15-1	3300.0	8.8	1.82
Araldite 2014-1	15	A15-2	3001.6	8.0	1.76
Araldite 2014-1	15	A15-3	2924.0	7.8	1.55
		Mean	**3075.2**	**8.2**	**1.71**
Araldite 2014-1	20	A20-1	2751.0	5.5	1.63
Araldite 2014-1	20	A20-2	3065.4	6.1	1.80
Araldite 2014-1	20	A20-3	2851.6	5.7	1.45
		Mean	**2889.3**	**5.8**	**1.63**
Araldite 2014-1	25	A25-1	2701.4	4.3	1.50
Araldite 2014-1	25	A25-2	2854.4	4.6	1.54
Araldite 2014-1	25	A25-3	2824.0	4.5	1.32
		Mean	**2793.3**	**4.5**	**1.45**
Araldite 2014-1	30	A30-1	2511.8	3.4	1.27
Araldite 2014-1	30	A30-2	2394.3	3.2	1.70
Araldite 2014-1	30	A30-3	2202.5	2.9	1.34
		Mean	**2369.6**	**3.2**	**1.44**
Carbon Kleber CG49	15	C15-1	4032.4	10.8	2.83
Carbon Kleber CG49	15	C15-2	4116.0	11.0	3.86
Carbon Kleber CG49	15	C15-3	3999.1	10.7	2.29
		Mean	**4049.1**	**10.8**	**2.99**
Carbon Kleber CG49	20	C20-1	5438.6	10.9	3.42
Carbon Kleber CG49	20	C20-2	5462.8	10.9	3.23
Carbon Kleber CG49	20	C20-3	5216.9	10.4	1.64
		Mean	**5372.8**	**10.7**	**2.76**
Carbon Kleber CG49	25	C25-1	5478.4	8.8	1.46
Carbon Kleber CG49	25	C25-2	5650.7	9.0	2.89
Carbon Kleber CG49	25	C25-3	5549.6	8.9	3.56
		Mean	**5559.6**	**8.9**	**2.64**
Carbon Kleber CG49	30	C30-1	5712.5	7.6	4.42
Carbon Kleber CG49	30	C30-2	5813.7	7.8	4.58
Carbon Kleber CG49	30	C30-3	5760.9	7.7	4.85
		Mean	**5762.3**	**7.7**	**4.62**

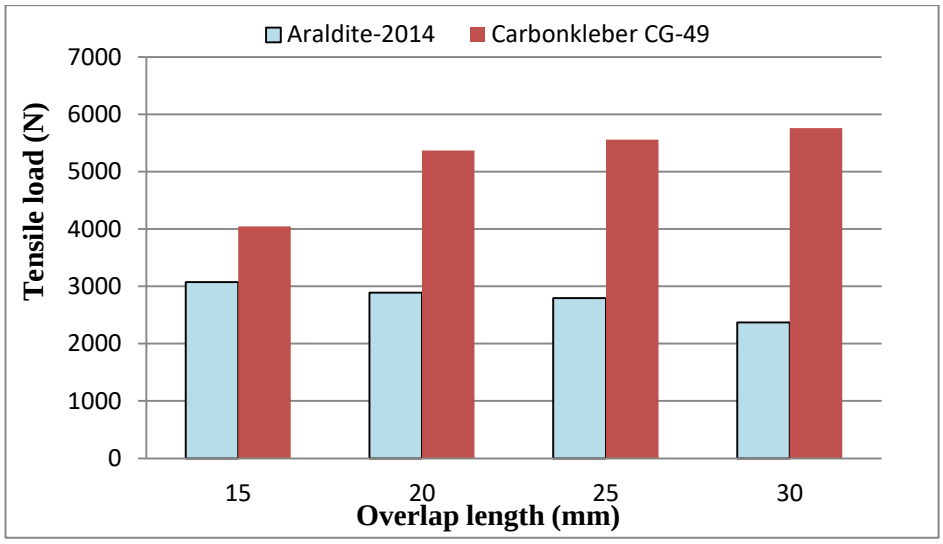

Figure 4.1 Average tensile load vs. overlap length for Mode I Test

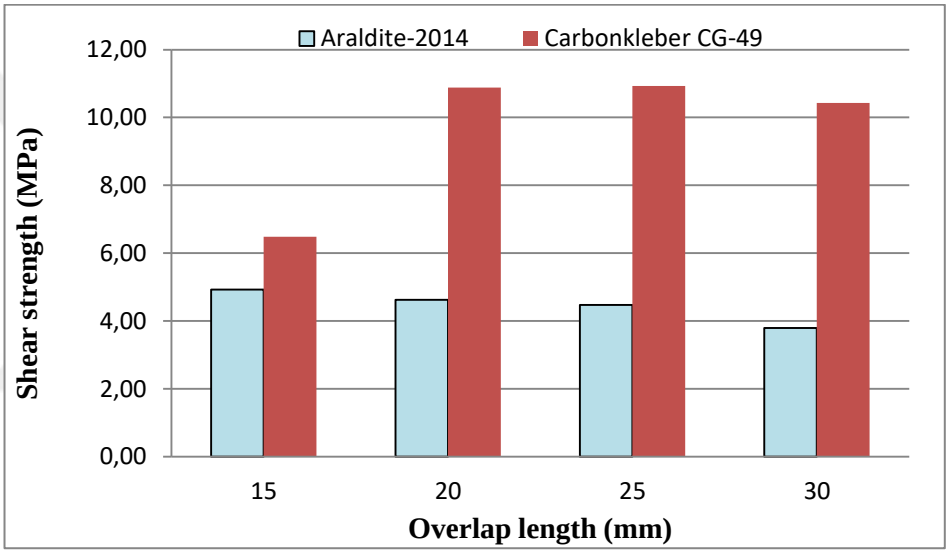

Figure 4.2 Average shear strength vs. overlap length for Mode I Test

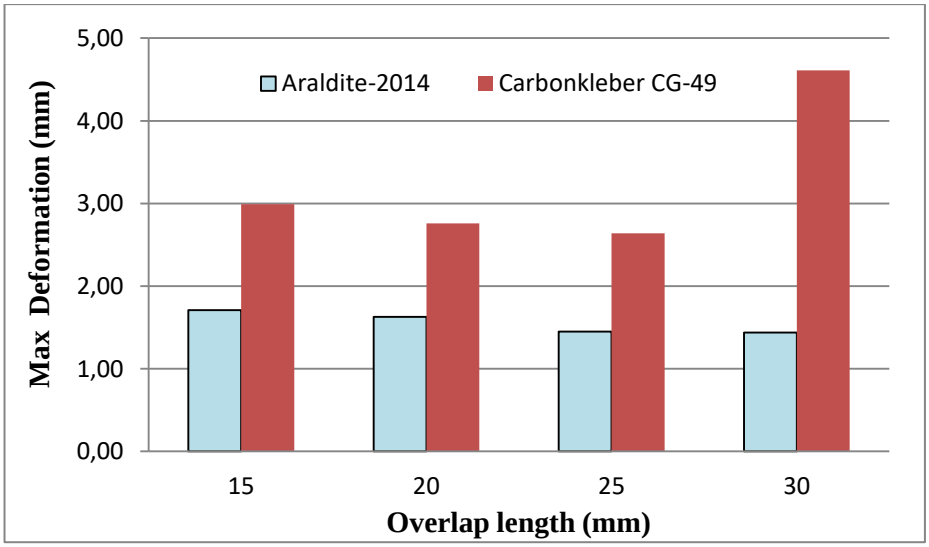

Figure 4.3 Maximum deformation (mm) vs. overlap length for Mode I Test

After the tensile tests the damage photos of the samples bonded with Araldite 2014-1 type adhesive are examined, it is seen that generally the adhesion type damages occur (Figures 4.4, 4.5, 4.6 and 4.7). It means that, the adhesive remained on either the aluminium plate or the GFRP plate. However, both adhesion type and cohesion type failure were seen on the damage photos of bonded samples with Carbon-Kleber type adhesive (Figures 4.8, 4.9, 4.10 and 4.11). These results suggest that Carbon-Kleber type adhesive is very strong. Furthermore obtained tensile load values of C20-1, C30-1 and C30-3 samples were 5438.6, 5712.5 and 5760.9 N respectively. However, the breakage occurred not from the adhesive but from the aluminium plates (see Figure 4.8, 4.9 and 4.11) at those samples. This result shows that Carbon-Kleber adhesive was stronger than aluminium plates. In order to determine strength in single lap bonding joints, not only adhesive but also adherent strength must be taken into account. Consequently, it can be said that the adhesion strength (Carbon-Kleber) is higher than the strength of Al-1050.

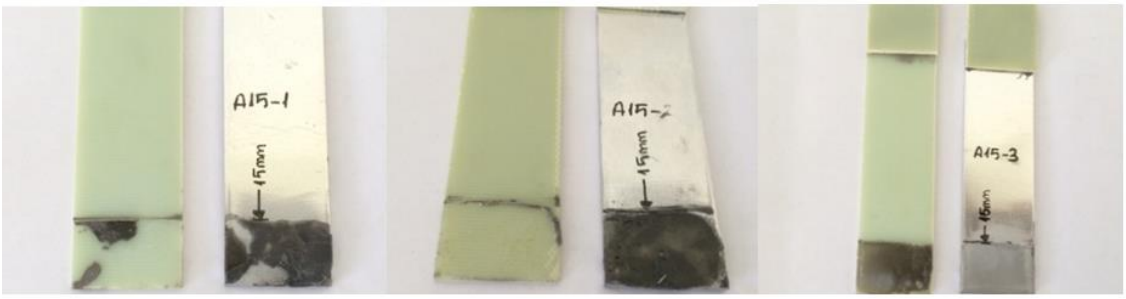

Figure 4.4 A15 Samples after tensile tests

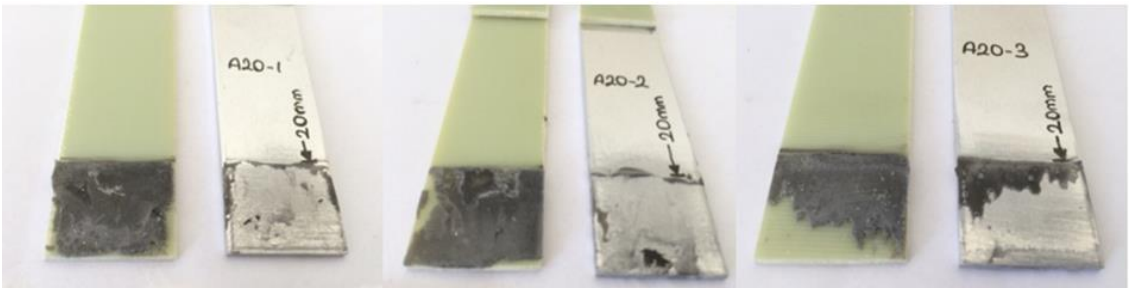

Figure 4.5 A20 Samples after tensile tests

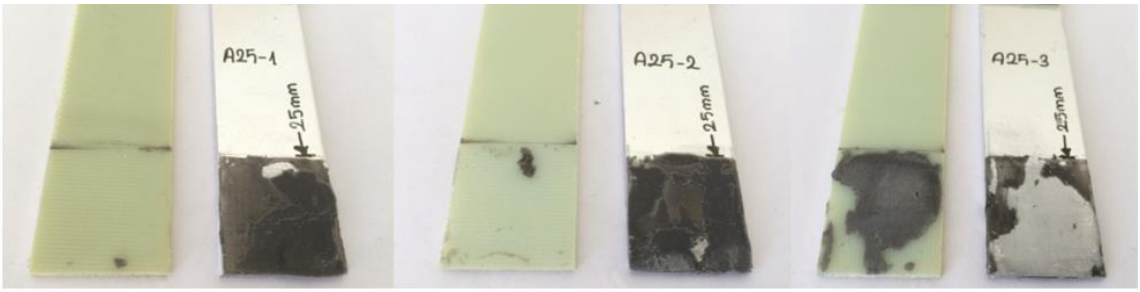

Figure 4.6 A25 Samples after tensile tests

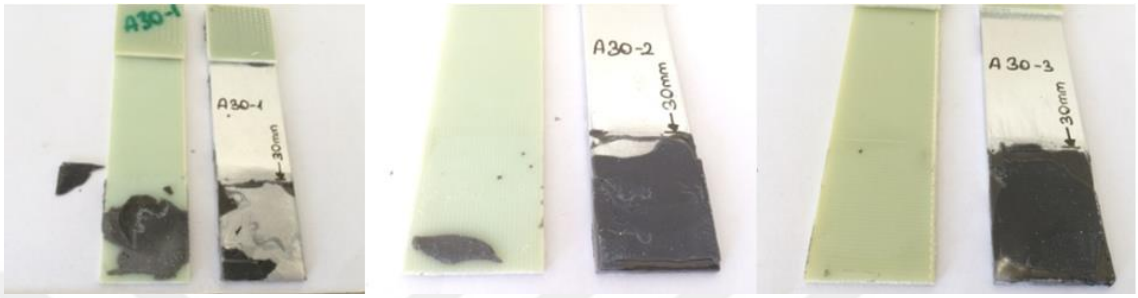

Figure 4.7 A30 Samples after tensile tests

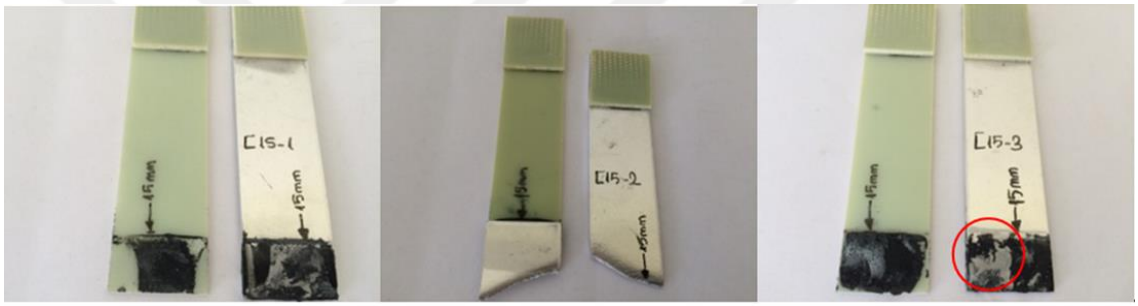

Figure 4.8 C15 Samples after tensile tests

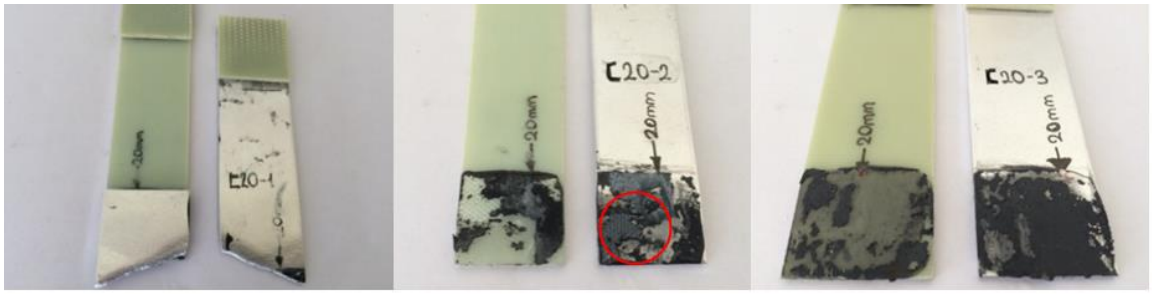

Figure 4.9 C20 Samples after tensile tests

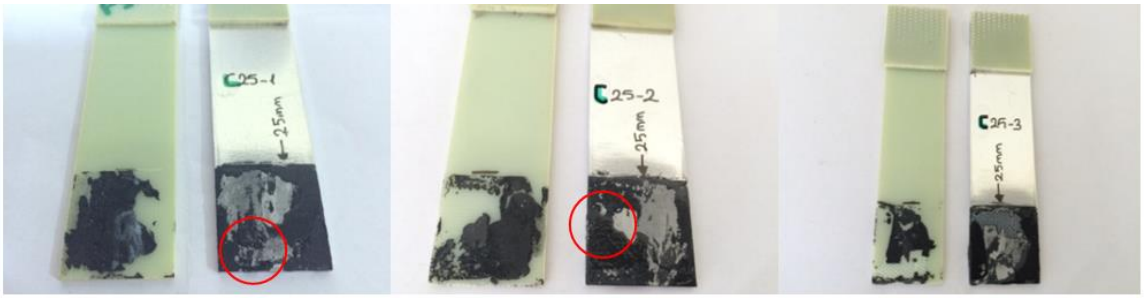

Figure 4.10 C25 Samples after tensile tests

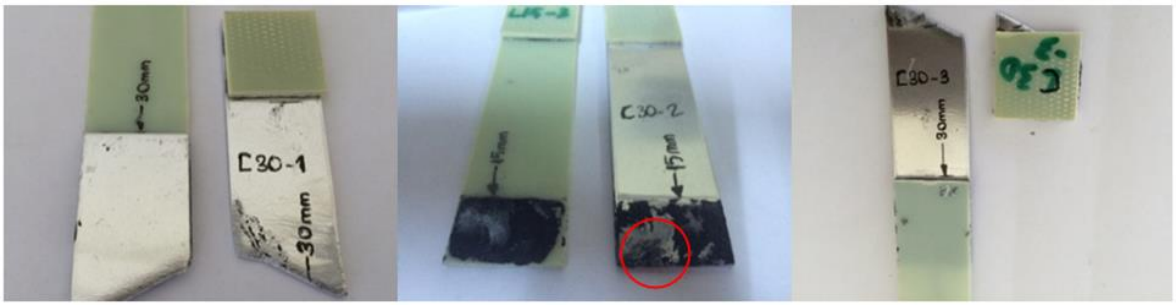

Figure 4.11 C30 Samples after tensile tests

Mode I test results showed that the Carbon-Kleber type adhesive was very strong, so it was decided to investigate how the nano-particle addition to Araldite-2014 type adhesive would affect the strength of Al and GFRP bonded joint.

4.2 Mode II Test Results

In Mode II tests, aluminium alloy 7075-T6 and G10-FR-4 plates were used as adherents with adhesives of Araldite 2014-1. In these experiments, a mould that was designed and constructed was used for properly adjusting the adhesive thickness and overlap length (25 mm). The specimens were prepared by adding 0.5%, 1% and 1.5% by weight of nano-silica and nano-clay particles to the adhesive by hand mixing. Obtained tensile loads and calculated shear strength results are given in Table 4.2.

Average tensile load, shear strength and deflection values were 2793.3N, 4.5 MPa, 1.45 mm with pure Araldite 2014 samples when overlap length was 25 mm (Table 4.1). The best tensile loads were obtained at a ratio of 0.5% by weight for both nano-particles (Figure 4.12). The maximum values of tensile load, shear strength and displacement were 3121.4 N, 4.99 MPa and 1.55 mm, for nano-silica reinforced samples. However, these values were 3941.9 N, 6.31 MPa and 1.80 mm for nano-clay reinforced samples. The maximum values were observed at 0.5% weight for both nano-particles. It was observed that as the ratio of nano-particles added to the adhesive increased, the tensile load decreased. Nano-clay reinforced samples have better tensile load, shear strength and displacement values than the nano-silica reinforced samples for all weight ratios (Figures 4.12, 4.13 and 4.15).

Table 4.2 Results of Mode II Test

Nano-Particle and Ratio		Specimen Code	Maximum Tensile Force (N)	Shear Strength (MPa)	Maximum Deflection (mm)
Nano-Silica	0.5%	0.5%NS-1	1813.46	2.90	1.63
Nano-Silica	0.5%	0.5%NS-2	3612.66	5.78	1.29
Nano-Silica	0.5%	0.5%NS-3	3323.13	5.32	1.26
Nano-Silica	0.5%	0.5%NS-4	4036.57	6.46	1.43
Nano-Silica	0.5%	0.5%NS-5	2821.06	4.51	2.14
Mean			**3121.4**	**4.99**	**1.55**
Nano-Silica	1%	1%NS-1	2339.13	3.74	0,80
Nano-Silica	1%	1%NS-2	2669.72	4.27	0,98
Nano-Silica	1%	1%NS-3	2324.53	3.72	1,19
Nano-Silica	1%	1%NS-4	2688.93	4.30	0,73
Nano-Silica	1%	1%NS-5	2576.83	4.12	1,03
Mean			**2519.8**	**4.03**	**0.95**
Nano-Silica	1.5%	1.5%NS-1	2052.88	3.28	0.50
Nano-Silica	1.5%	1.5%NS-2	2166.7	3.47	0.67
Nano-Silica	1.5%	1.5%NS-3	561.571	0.90	0.16
Nano-Silica	1.5%	1.5%NS-4	1740.12	2.78	0.60
Nano-Silica	1.5%	1.5%NS-5	1986.57	3.18	0.65
Mean			**1701.57**	**2.72**	**0.61**
Nano-Clay	0.5%	0.5%NC-1	2867.03	4.59	1.24
Nano-Clay	0.5%	0.5%NC-2	4796.65	7.67	3.10
Nano-Clay	0.5%	0.5%NC-3	4851.77	7.76	1.52
Nano-Clay	0.5%	0.5%NC-4	3542.57	5.67	1.90
Nano-Clay	0.5%	0.5%NC-5	3651.43	5.84	1.23
mean			**3941,9**	**6.31**	**1.80**
Nano-Clay	1%	1%NC-1	2848.58	4.56	0.92
Nano-Clay	1%	1%NC-2	3441.05	5.51	1.14
Nano-Clay	1%	1%NC-3	2576.21	4.12	0.63
Nano-Clay	1%	1%NC-4	2663.66	4.26	1.05
Nano-Clay	1%	1%NC-5	2197.7	3.52	2.64
Mean			**2745,4**	**4.39**	**1.28**
Nano-Clay	1.5%	1.5%NC-1	2050.35	3.28	0.66
Nano-Clay	1.5%	1.5%NC-2	1853.42	2.97	0.67
Nano-Clay	1.5%	1.5%NC-3	2738.67	4.38	0.57
Nano-Clay	1.5%	1.5%NC-4	2419.76	3.87	0.96
Nano-Clay	1.5%	1.5%NC-5	2541.59	4.07	1.18
Mean			**2320,8**	**3.71**	**0.81**

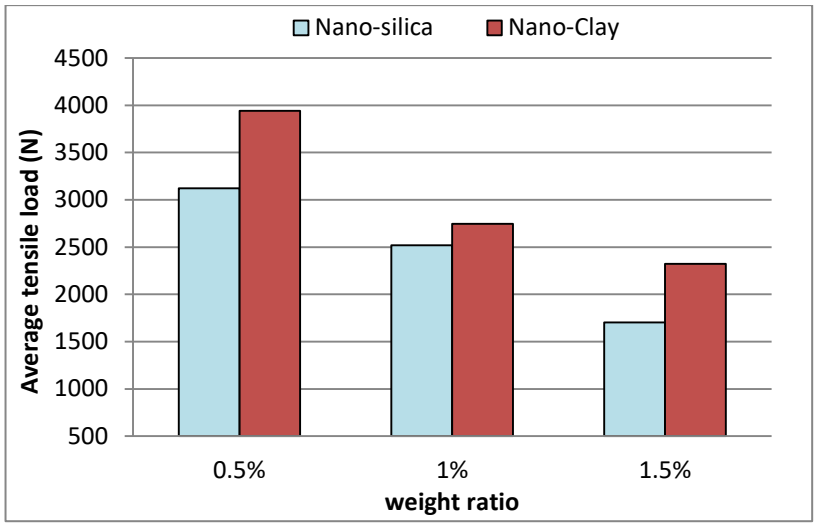

Figure 4.12 Average tensile load vs. nano-particles ratio for Mode I Test

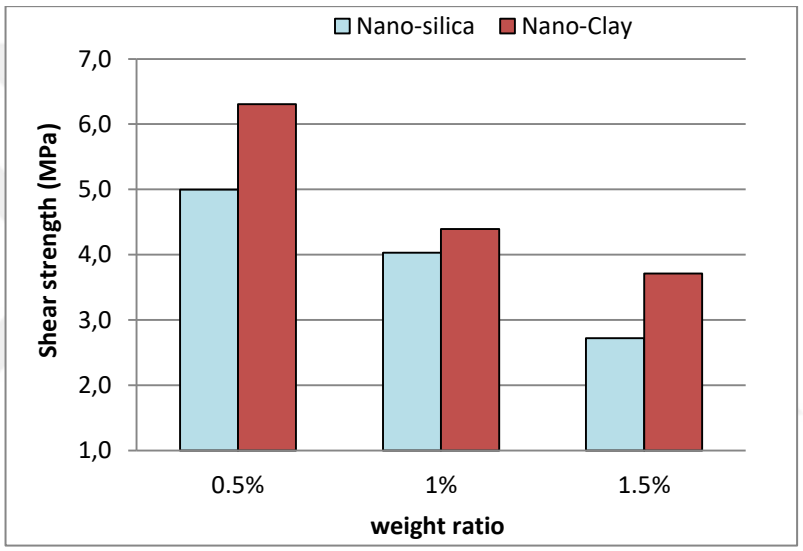

Figure 4.13 Shear strength values vs. nano-particles ratio for Mode I Test

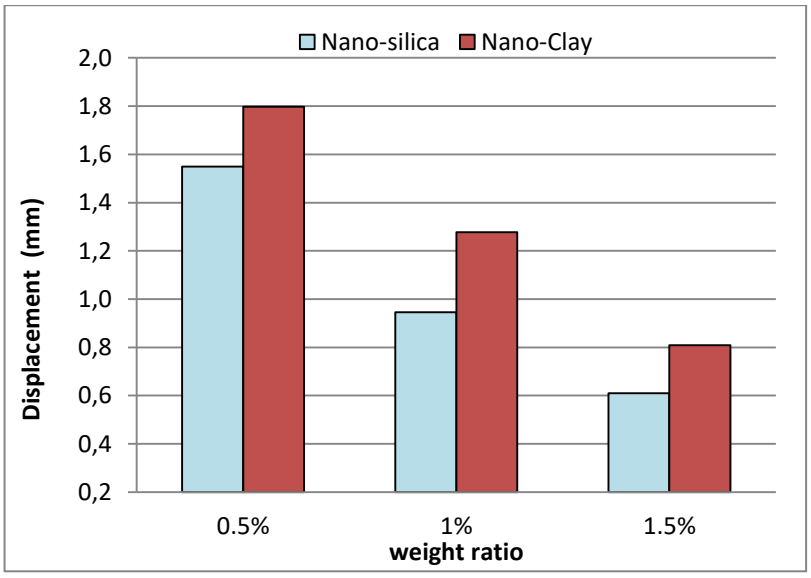

Figure 4.14 Average displacement values vs. nano-particles ratio for Mode I Test

Figure 4.15 shows the images of the samples pasted with neat Araldite 2014-1, after the tensile test. When the bonding surfaces are examined, it is seen that adhesive either adhered to the glass fibre plate or the aluminium side, that is, adhesion type breakage. However, nano-clay doped samples after tensile tests have cohesive type failure (see Figure 4.16). Moreover, when the damaged surfaces of nano-silica added samples are examined, both adhesive and cohesive type deterioration are seen together (Fig. 4.17). Cohesion-induced damage (detachment of the adhesive layer) indicates that the nano-particle addition to adhesive enhances the adhesive's ability to adherent plates. It was seen that in Mode II test, adding more than 0.5% of the nano-particles to adhesive causes agglomeration in the adhesive due to manual mixing.

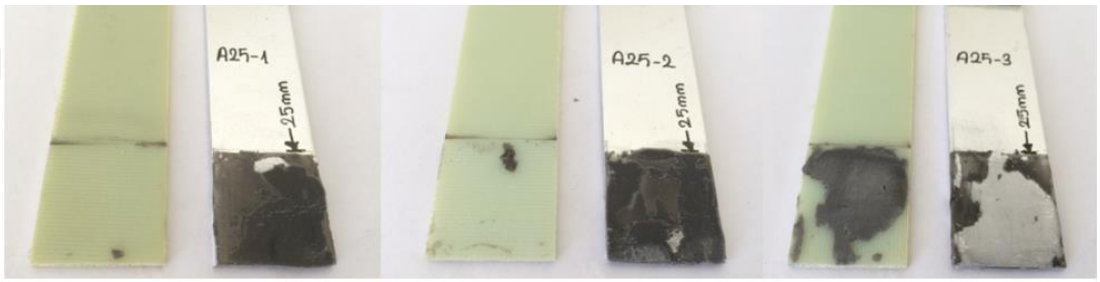

Figure 4.15 Appearance of bonding surfaces with pure Araldite bonded samples after tensile tests

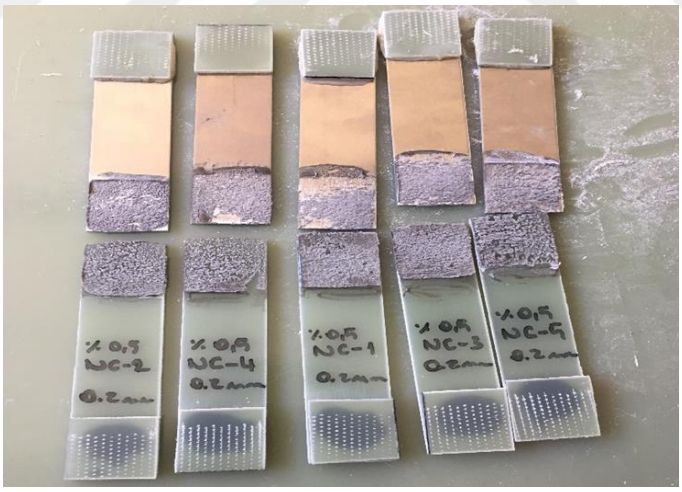

Figure 4.16 Appearance of bonding surfaces of nano-clay doped samples after tensile tests

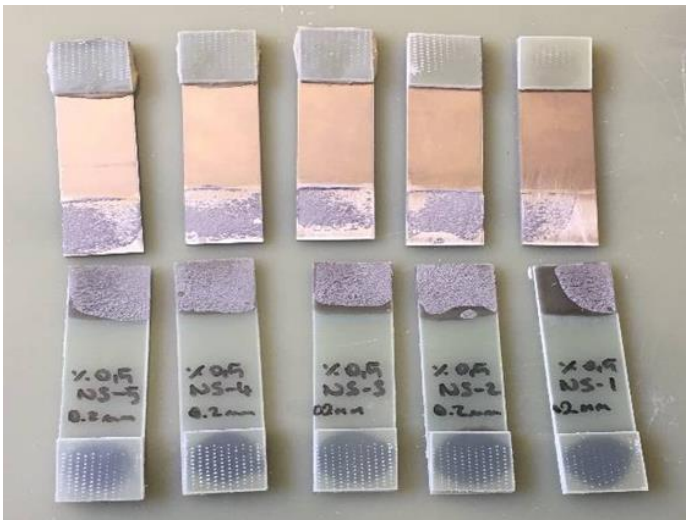

Figure 4.17 Appearance of bonding surfaces of nano-silica doped samples after tensile tests

4.3 Mode III Test Results

In Mode III test, it was aimed to increase the mechanical properties of bonding joints of Aluminium 2024-T3 and GFRP sheets by using MWCNT (multi-walled carbon nano-tube) added to commercial adhesive Araldite 2014-1. The single lap joints specimens were prepared by adding 0.25%, 0.5%, 1%, 1.5% and 2% by weight of MWCNT to Araldite 2014 epoxy adhesive. To prevent agglomeration, the highly viscous adhesive was mixed with a 1:1 ratio of Merck 100014 brand acetone (C_3H_6O) in 99% purity and it was mixed with a light load homogenizer at 22,000 rpm for 30 minutes (Figure 3.26-B). Firstly, adhesively bonded samples with neat Araldite 2014-1 were tested to compare the effect of MWCNT addition and results are given at Table 4.3. The results of the tensile tests of MWCNT added samples are seen at Table 4.4.

Table 4.3 Test results of samples pasted with pure Araldite-2014-1

Adhesive	Nano-Particle	Specimen Code	Maximum Tensile Force (N)	Shear Strength (MPa)	Max Deformation (mm)
Araldite 2014-1	**None**	**P1**	4697.8	7.5	1.20
Araldite 2014-1	**None**	**P2**	5141.7	8.2	1.80
Araldite 2014-1	**None**	**P3**	5915.2	9.5	2.20
Araldite 2014-1	**None**	**P4**	4749.3	7.6	1.60
Araldite 2014-1	**None**	**P5**	5633.3	9.0	1.20
Mean			**5227.5**	**8.4**	**1.60**

Table 4.4 Results of Mode III Tests

Nano-Particle	Specimen Code	Tensile load (N)	Shear Strength (MPa)	Max. Deformation (mm)
0.25wt. % MWCNT	**C0-1**	7856.85	12.57	1.51
0.25wt. % MWCNT	**C0-2**	7329.37	11.73	1.49
0.25wt. % MWCNT	**C0-3**	7907.15	12.65	1.86
0.25wt. % MWCNT	**C0-4**	6990.86	11.19	1.55
0.25wt. % MWCNT	**C0-5**	8528.33	13.65	1.76
Mean		**7722.51**	**12.36**	**1.63**
0.5wt. % MWCNT	**C1-1**	8569.34	13.71	1.62
0.5wt. % MWCNT	**C1-2**	8683.73	13.89	2.07
0.5wt. % MWCNT	**C1-3**	8154.63	13.05	1.92
0.5wt. % MWCNT	**C1-4**	8657.69	13.85	2.02
0.5wt. % MWCNT	**C1-5**	8333.25	13.33	1.72
Mean		**8479.73**	**13.57**	**1.87**
1wt. % MWCNT	**C2-1**	7243.78	11.59	1.8
1wt. % MWCNT	**C2-2**	8333.25	13.33	1.89
1wt. % MWCNT	**C2-3**	7633.35	12.21	1.46
1wt. % MWCNT	**C2-4**	8055.21	12.89	1.93
1wt. % MWCNT	**C2-5**	7441.04	11.91	1.96
Mean		**7741.33**	**12.39**	**1.81**
1.5wt. % MWCNT	**C4-1**	6902.79	11.04	0.95
1.5wt. % MWCNT	**C4-2**	7610.46	12.18	1.46
1.5wt. % MWCNT	**C4-3**	7372.28	11.80	1.32
1.5wt. % MWCNT	**C4-4**	5656.05	9.05	1.18
1.5wt. % MWCNT	**C4-5**	7439.14	11.90	1.88
Mean		**6996.14**	**11.19**	**1.36**
2wt. % MWCNT	**C3-1**	7197.38	11.52	1.6
2wt. % MWCNT	**C3-2**	6272.55	10.04	1.27
2wt. % MWCNT	**C3-3**	6515.22	10.42	1.15
2wt. % MWCNT	**C3-4**	5067.4	8.11	1.09
2wt. % MWCNT	**C3-5**	6401.54	10.24	1.27
Mean		**6290.82**	**10.07**	**1.28**

In 0.25% by wt. MWCNT reinforced connections, the tensile load increased at about 50%. Maximum tensile load (8479.72 N) was obtained as 62% at 0.5% by wt. After this ratio, the tensile load has reduced (Table 4.4).

As seen in Figure 4.19, the shear strength increased up to maximum 13.57 MPa (at 0.5% by wt. MWCNT) and after reaching the maximum value, the improvement

begun to decrease. Furthermore, when the results of displacement are taken into consideration, it is 1.6 mm in the pure adhesive joints, while it is 1.87 mm in the adhesive joints with 0.5% MWCNT by weight. This demonstrates that the addition of MWCNT also improves the ductility of the adhesive.

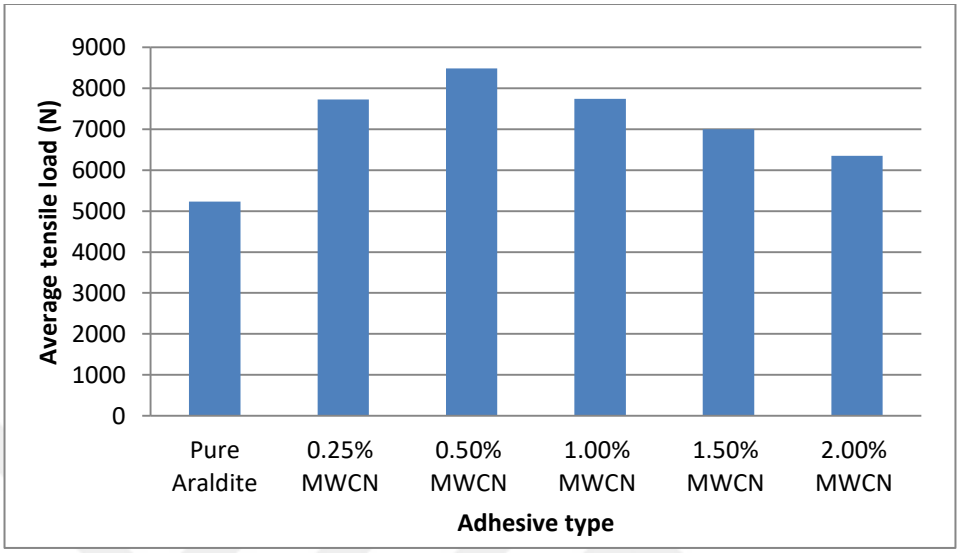

Figure 4.18 Graph of average tensile loads vs. adhesive types for Mode III test

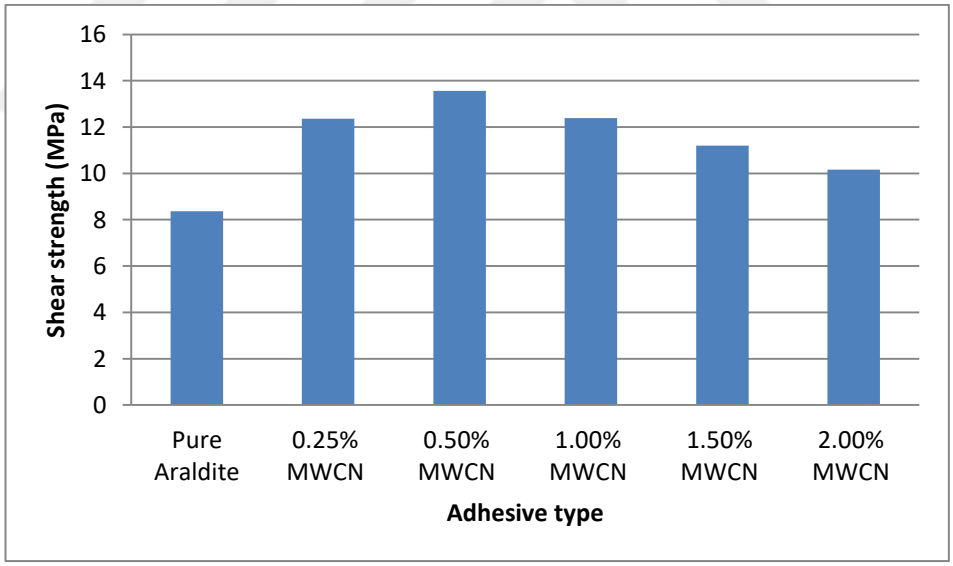

Figure 4.19 Graph of average shear stress vs. adhesive types for Mode III test

When the bonding surfaces after tensile test are examined, it is seen that the adhesive remains on a single surface of pure Araldite samples (Figure 4.20). It means that, adhesion type failure was realized. After the tensile tests, when the specimens of the MWCNT doped joints are visually inspected, both adhesion and cohesion type failure were observed together (Fig. 4.21). In between 0.25 to 1% by weight MWCNT doped connections, it was observed that the adhesive penetrates better into

both Al and GFRP sheet, so that the cohesion type breakage increased (Figure 4.21-a, b and c). After 1.5% additive ratio, it was seen that there were pores in the form of air gaps in the connection surfaces. These pores reduce the adsorption and thus the fracture strength decreases. This is due to the increase in surface tension of the CNTs and the adhesion of the adhesive to the CNT surfaces rather than the plates.

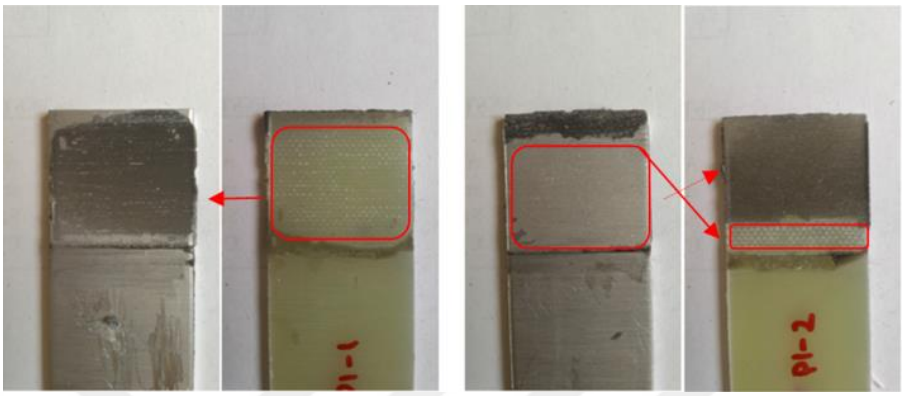

Figure 4.20 Views of adhesive type failure on pure Araldite samples

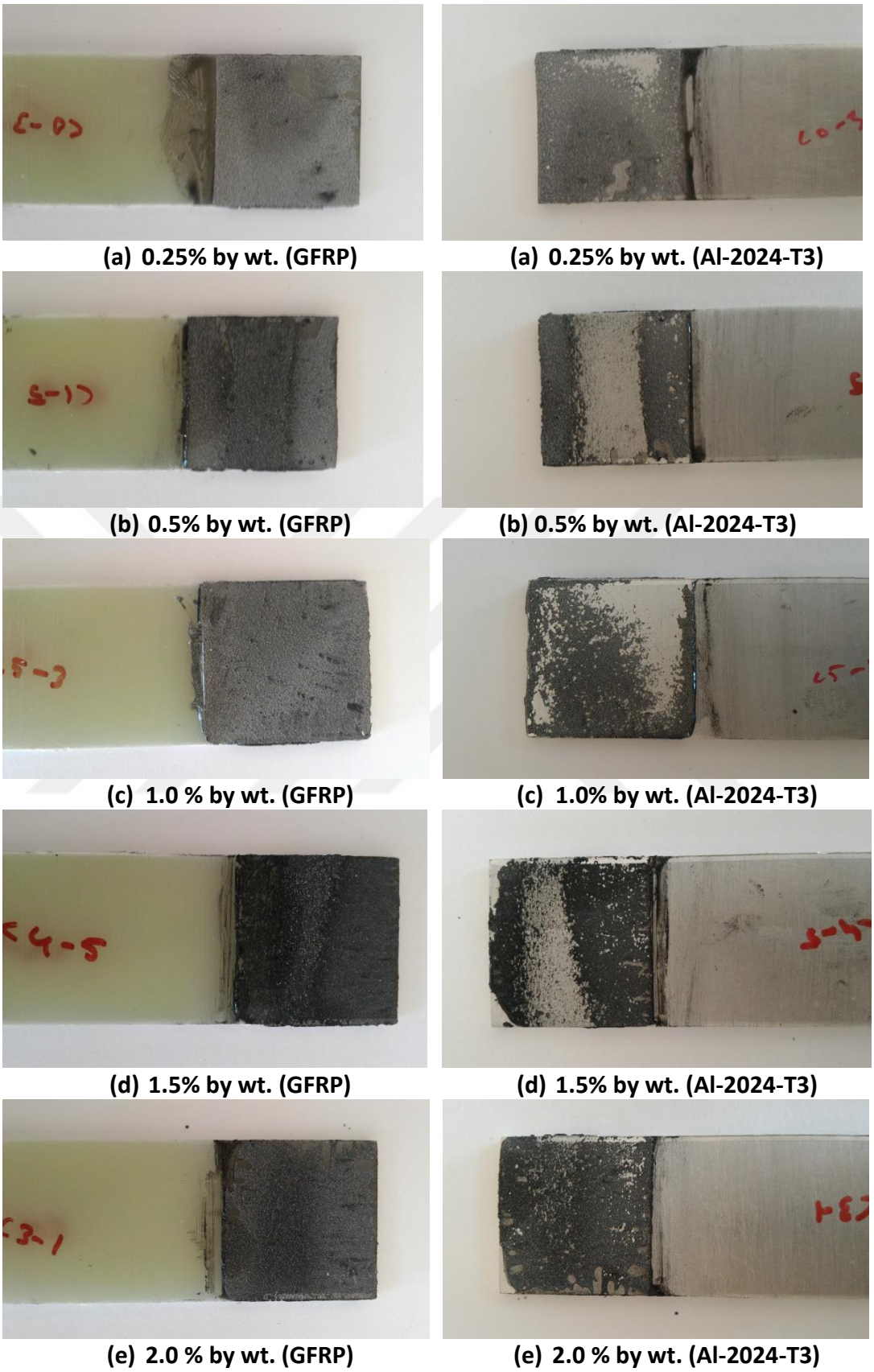

(a) 0.25% by wt. (GFRP) (a) 0.25% by wt. (Al-2024-T3)

(b) 0.5% by wt. (GFRP) (b) 0.5% by wt. (Al-2024-T3)

(c) 1.0 % by wt. (GFRP) (c) 1.0% by wt. (Al-2024-T3)

(d) 1.5% by wt. (GFRP) (d) 1.5% by wt. (Al-2024-T3)

(e) 2.0 % by wt. (GFRP) (e) 2.0 % by wt. (Al-2024-T3)

Figure 4.21 Views of bonding surfaces of MWCNT doped samples after tensile tests

4.4 Mode IV Test Results

In this mode, effect of nano-silica particles on shear strength and impact behaviour of AL-GFRP bonding joints was investigated. Shear performance of bonding samples were researched by universal tensile test machine in accordance to ASTM D 3039 international standards. Charpy impact test was used to evaluate the impact performances of samples in accordance to ISO 179 international standards.

4.4.1 Results of the Tensile Tests for Mode IV

Tensile test results are given at Table 4.5. It is seen that the nano-silica additive generally improves the bond strength (Figure 4.22 and 4.23). While the average shear strength of the unadulterated samples is 8.36 MPa, shear strength of samples with 0.5% by weight reaches 10.04 MPa. Samples doped with 1.5% by weight have the best tensile load and shear strength values with an increase of 43.3%. When the nano-silica added samples are visually inspected after the experiment, it is understood that the damage is due to cohesion (detachment of the adhesive layer), that is to say the adhesive is well fastened on the glass fibre and Al plates (Figure 4.24). Addition of 0.5% to 1.5% of nano-silica particles to the adhesive creates a film structure that increases the effective contact area and causes the adhesive to increase the cohesion resistance. However, adding 2% by wt. nano-silica contribution causes agglomeration of the particles. This agglomeration can lead to a sudden break in the bond, caused by stress concentration and cracks in the adhesive layer even under low stresses.

Table 4.5 Tensile test results of Mode IV test

Nano-Particle and weight rate	Specimen Code	Tensile Load (N)	Shear Strength (MPa)	Deformation (mm)
0.5wt. % Silica	**A1-1**	6148.3	9.8	2.0
0.5wt. % Silica	**A1-2**	6357.5	10.2	2.1
0.5wt. % Silica	**A1-3**	6450.5	10.3	2.3
0.5wt. % Silica	**A1-4**	6268.5	10.0	1.8
0.5wt. % Silica	**A1-5**	6154.9	9.8	1.7
Mean		**6275.9**	**10.0**	**2.0**
1wt. % Silica	**A2-1**	7938.7	12.7	2.3
1wt. % Silica	**A2-2**	6953.0	11.1	1.9
1wt. % Silica	**A2-3**	7012.9	11.2	2.2
1wt. % Silica	**A2-4**	6897.7	11.0	2.1
1wt. % Silica	**A2-5**	6006.0	9.6	1.9
Mean		**6961.7**	**11.1**	2.1
1.5wt. % Silica	**A3-1**	7702.8	12.3	3.2
1.5wt. % Silica	**A3-2**	6387.2	10.2	2.5
1.5wt. % Silica	**A3-3**	7663.7	12.3	2.4
1.5wt. % Silica	**A3-4**	7426.6	11.9	1.8
1.5wt. % Silica	**A3-5**	8273.5	13.2	2.4
Mean		**7490.8**	**12.0**	**2.4**
2wt. % Silica	**A4-1**	6950.2	11.1	2.8
2wt. % Silica	**A4-2**	6548.0	10.5	2.3
2wt. % Silica	**A4-3**	6268.5	10.0	1.9
2wt. % Silica	**A4-4**	7702.8	12.3	2.5
2wt. % Silica	**A4-5**	6671.5	10.7	2.5
Mean		**6828.2**	**10.9**	**2.4**

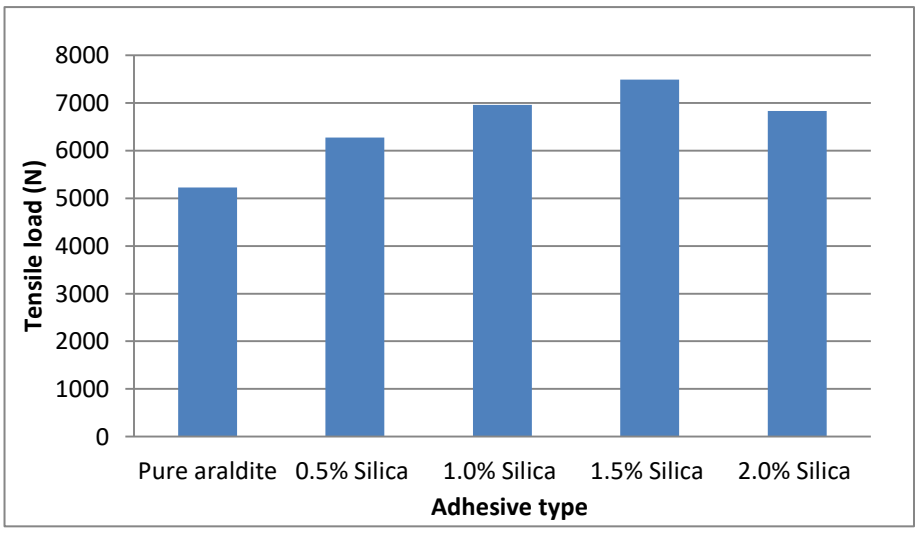

Figure 4.22 Graph of average tensile loads vs. adhesive types for Mode IV test

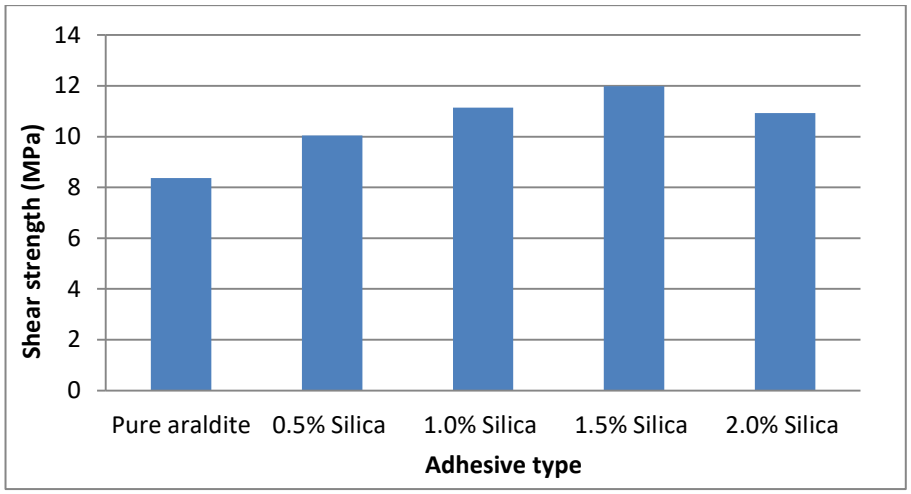

Figure 4.23 Graph of average shear stress vs. adhesive types for Mode IV test

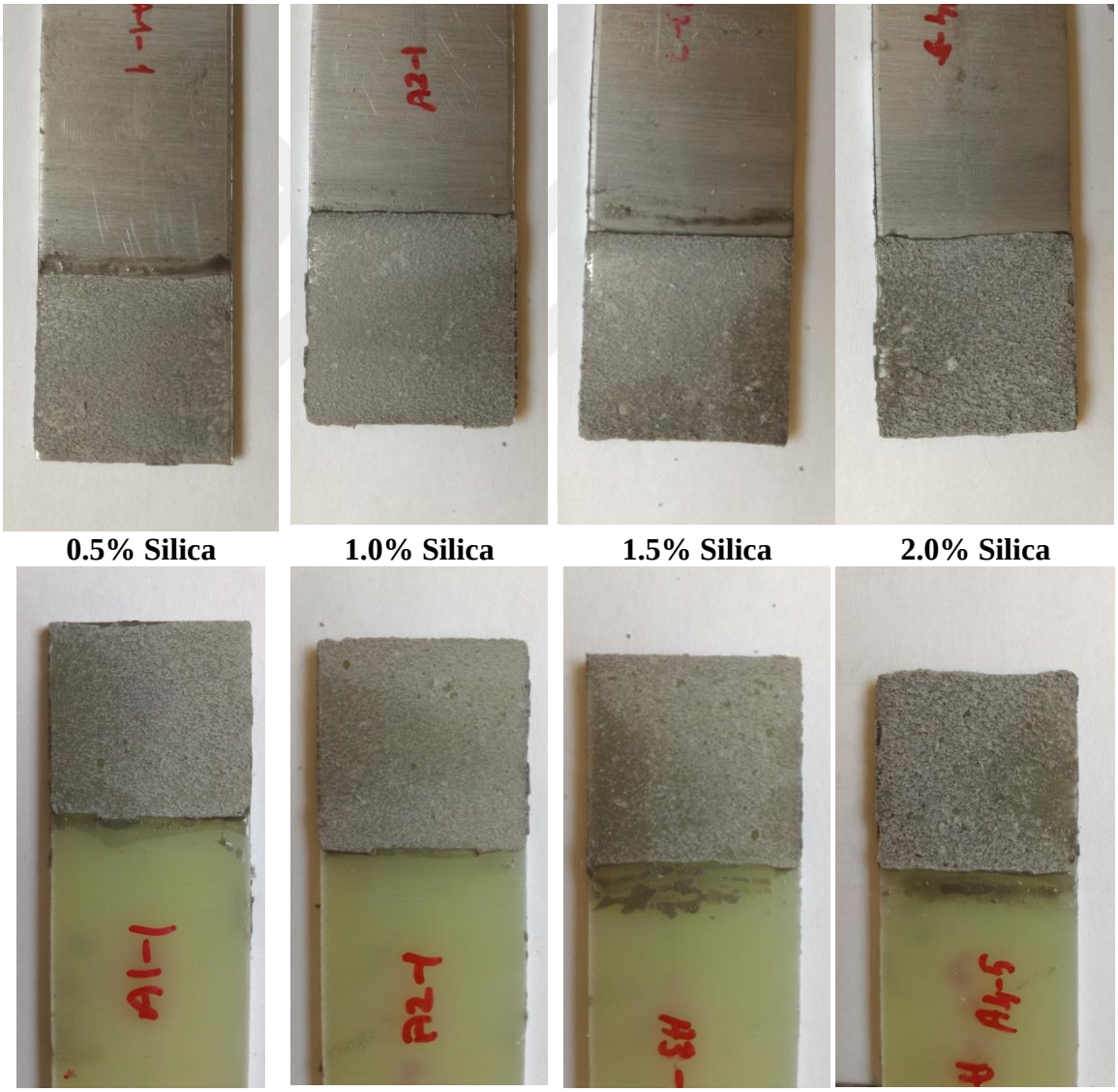

Figure 4.24 Apperances of damage surfaces of nano-silica doped samples on Al and GFRP plates

4.4.2 Results of the Charpy Impact Tests for Mode IV

In this test, 5 different types of specimens were prepared and totally 50 experiments were carried out by Kögel 3/70 Charpy impact tester equipped with impact load with 15J. In the impact test, the energy absorbed during fracture is used as a measure of the brittleness or impact resistance of the material. The findings of the Charpy impact tests are given in Table 4.6 (for Al direction) and Table 4.7 (for GFRP direction) as mean impact energy and impact toughness.

Table 4.6 Charpy impact test results of nano-silica doped adhesive connections (Al direction)

Adhesive type	Impact Energy (Joule)					Mean Impact Energy (Joule)	Impact Toughness a_{cu} (kj/m^2)
	Sample No						
	1	2	3	4	5		
Pure Araldite	3.6	3.3	3	4.3	3.5	3.54	15.32
0.5% Silica	3.1	4.0	3.7	3.2	3.8	3.56	15.41
1.0 % Silica	3.5	3.3	3.9	3.2	4.0	3.58	15.5
1.5% Silica	3.9	4.0	3.0	3.8	3.5	3.64	15.76
2.0 % Silica	3.4	3.5	3.7	3.6	3.5	3.54	15.32

Table 4.7 Charpy impact test results of nano-silica doped adhesive connections (GFRP direction)

Adhesive type	Impact Energy (Joule)					Mean Impact Energy (Joule)	Impact Toughness a_{cu} (kj/m^2)
	Sample No						
	1	2	3	4	5		
Pure Araldite	4.3	4.3	4.3	3.6	3.6	4.02	17.4
0.5% Silica	3.9	4.0	4.0	3.9	4.5	4.06	17.58
1.0 % Silica	3.8	4.0	4.0	4.5	4.5	4.16	18.01
1.5% Silica	4.6	4.3	4.6	4.3	4.5	4.46	19.31
2.0 % Silica	3.1	4.1	4.6	4.0	4.4	4.04	17.49

Impact energy differs according to impact direction. Looking at the test results from the Al orientation (Table 4.7 and Figure 4.25); it appears that the nano-silica particle addition does not significantly affect the impact energy of bonding. Impact energy increased by maximum 3% for Al side whereas Nano-silica doped by 1.5 %.

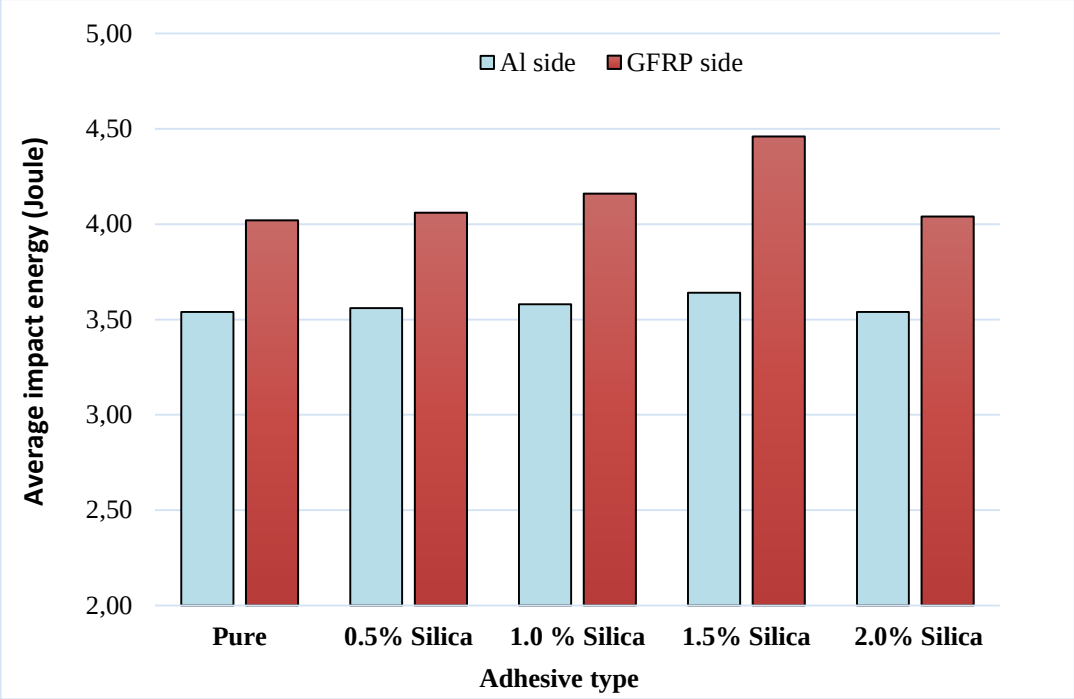

Figure 4.25 Charpy impact energy vs Al and GFRP direction

In the impact tests made by GFRP direction, the addition of 0.5%, 1% and 1.5% nano-silica improved the impact energy and toughness by 1%, 3.5% and 10.9% respectively (Table 4.7 and Figure 4.25). Bell and Kinloch [62] point out that the impact energy absorbed by the impact direction depends on the degree of transverse elasticity modulus and plastic deformation of the underlying layer.

When the photographs (Figure 4.26) obtained after the impact test are examined, it is seen that damage of samples is affected by the bottom plate material made of Al or glass fibre. In Figure 4.26, “G” label means GFRP plate is on the front, “A” label means Al plate is on the front PG means unadulterated samples, and AG1, AG2, AG3 and AG4 means 0.5%, 1%, 1.5% and % 2 silica added samples, respectively.

In the experiments conducted with Al plate direction, it is seen that the samples adhered with the pure adhesive are mostly separated from each other (Figure 4.26 “P”). In the nano-silica doped samples, the Al-GFRP plates are not separated from each other, that is, there is no rupture in the adhesive layer (Figure 4.26 “A1, A2, A3 and A4”).

Figure 4.26 Damages' views after Charpy impact test for nano-silica doped samples

In tests where the glass fibre plate is on the front (Figure 4.26 "G"); the GFRP plate and adhesive layer are subjected to compressive load along the thickness due to pressing by anvil from bottom and impactor from top. On GFRP plates, fibre breakage was occurred due to compressive load in the direction of impact. It has been observed that both Al and GFRP plates was broken in joints with pure Araldite due to the plastic change of the Al plate, and that the fracture is in the form of adhesion deterioration (Figure 4.26 "PG" and Figure 4.27-A). In the nano-silica doped joints (up to 1.5% by weight in Figure 4.26-AG1, AG2 and AG3), it is seen that only a part of the GFRP plate is broken and the separation is in the form of cohesion failure (Figure 4.27-B). In general, Al plates exposed to less plastic deformation in experiments where GFRP plates are on the front. This is due to the fact that the fibres in the GFRP plates can absorb a small portion of the impact energy and thus benefit to the Al plate. Even if the glass fibre layers break in small deviations, they can withstand applied loads due to relatively high membrane hardness, so that the Al plate can resist more deformation reliably.

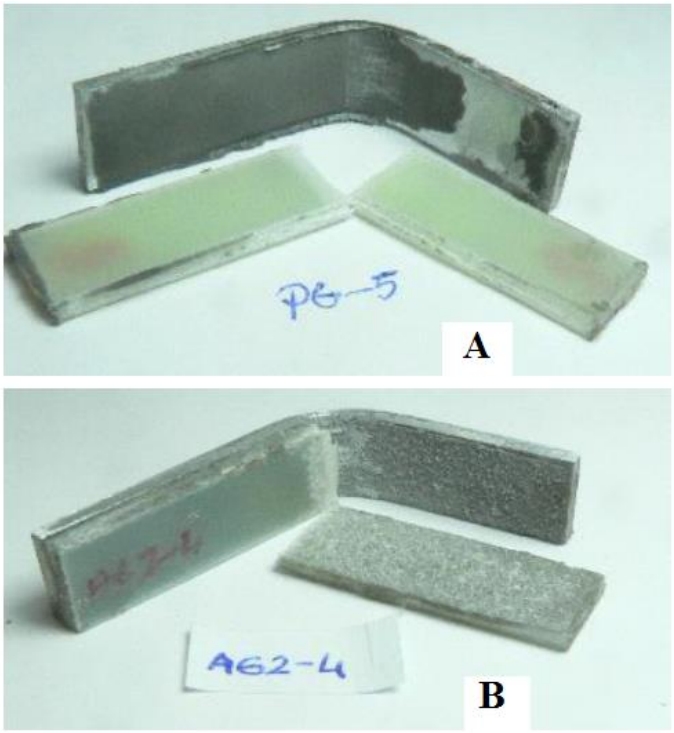

Figure 4.27 GFRP side damage (A) pure adhesive (B) nano-silica reinforced

4.5 Mode V Test Results

This study investigates the role of the addition of nano-clay particles to epoxy adhesive on the shear strength and impact strength of Al and GFRP bonding joints. Nano-clay particles were used as additive material within the epoxy adhesive by the weight ratios of 0.5, 1, 1.5 and 2.0 %.

4.5.1 Tensile Test Results of Mode V Test

Tensile test results (Table 4.8) showed that addition of nano-clay particles give enhancements in the shear performance of Al-GFRP adhesively bonded joint. While the average tensile load of the joints with pure Araldite is 5227.5 N, the obtained tensile load of nano-clay doped samples is 6566.5 N [minimum], i.e., the tensile load of the joint increased by 25.6%. The adhesion strength of nano-clay doped joints increased by 25.6, 35.0, 37.8, and 32.2% compared with the joints made with the unadulterated Araldite 2014-1. Based on the test results (Table 4.8 and Figure 4.29), it is seen that the maximum shear stress is 11.53 MPa in 1.5% nano-clay doped joints. After 1.5% nano-clay addition, shear strength tends to decrease (Figure 4.29).

Table 4.8 Tensile test results of Mode IV test

Adhesive type	Specimen Code	Tensile load (N)	Shear Strength (MPa)	Max Deformation (mm)
0.5% Clay	**B1-1**	6551.50	10.48	2.26
0.5% Clay	**B1-2**	6466.29	10.35	1.79
0.5% Clay	**B1-3**	6532.62	10.45	1.88
0.5% Clay	**B1-4**	6733.99	10.77	1.97
0.5% Clay	**B1-5**	7298.52	11.68	1.99
Mean		**6716.58**	**10.75**	**1.97**
1.0% Clay	**B2-1**	7328.61	11.73	2.14
1.0% Clay	**B2-2**	7398.94	11.84	2.60
1.0% Clay	**B2-3**	7707.88	12.33	1.94
1.0% Clay	**B2-4**	6986.33	11.18	1.84
1.0% Clay	**B2-5**	6564.67	10.50	2.28
Mean		**7197.29**	**11.52**	**2.16**
1.5% Clay	**B3-1**	6721.59	10.75	2.08
1.5% Clay	**B3-2**	6967.88	11.15	2.20
1.5% Clay	**B3-3**	7385.11	11.82	3.46
1.5% Clay	**B3-4**	7426.64	11.88	2.19
1.5% Clay	**B3-5**	7515.48	12.02	2.19
Mean		**7203.34**	**11.53**	**2.42**
2.0% Clay	**B4-1**	6936.46	11.10	2.06
2.0% Clay	**B4-2**	7790.76	12.47	2.13
2.0% Clay	**B4-3**	7248.50	11.60	2.00
2.0% Clay	**B4-4**	6598.00	10.56	2.44
2.0% Clay	**B4-5**	6945.47	11.11	2.08
Mean		**7103.83**	**11.37**	**2.14**

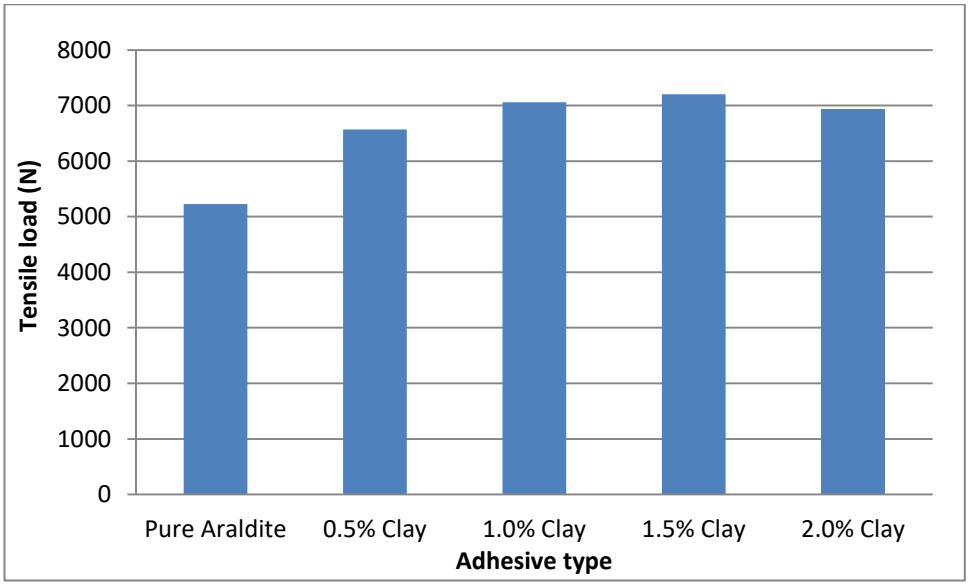

Figure 4.28 Graph of average tensile loads vs. adhesive types for Mode V test

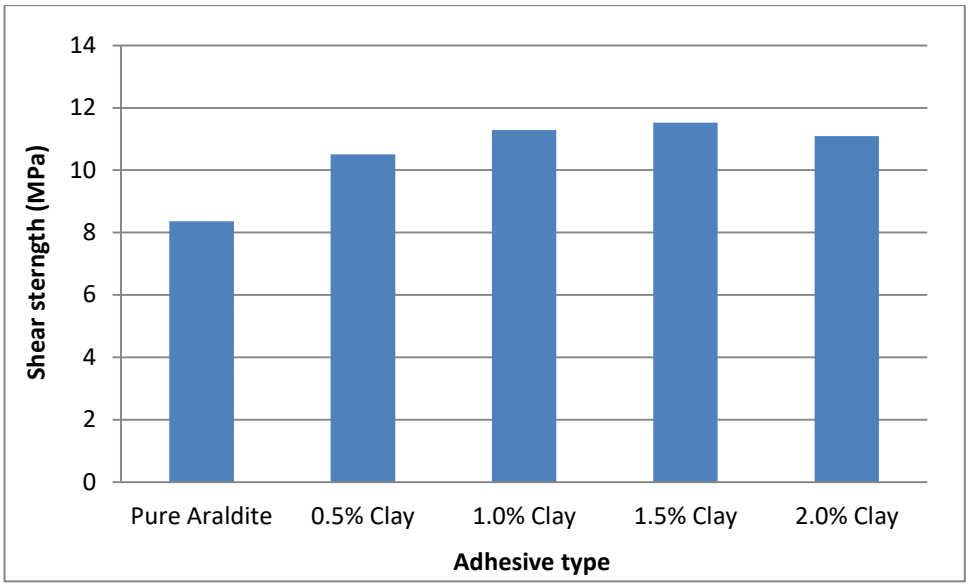

Figure 4.29 Graph of average shear stress vs. adhesive types for Mode V test

After the tensile tests, when the specimens are visually inspected, the difference in adhesion type deterioration is remarkable between the pure Araldite samples and the nano-clay doped samples (see Figure 4.30). In the unadulterated samples, the adhesiveness of the adhesive is low and there is a large amount of adhesion damage in the sample surfaces. Increasing the ratio of nano-clay in the adhesive causes the damage type to turn into cohesion damage. While at 0.5% and 1.0% nano-clay doped joints, cohesion damage is observed in large proportions, adhesion damage is also present. In the case of 2.0% nano-clay doped samples, as can be seen in Figure 4.30, the roughness on the surface of the adhesive increases, and in this respect, the adhesive property of the adhesive decreases.

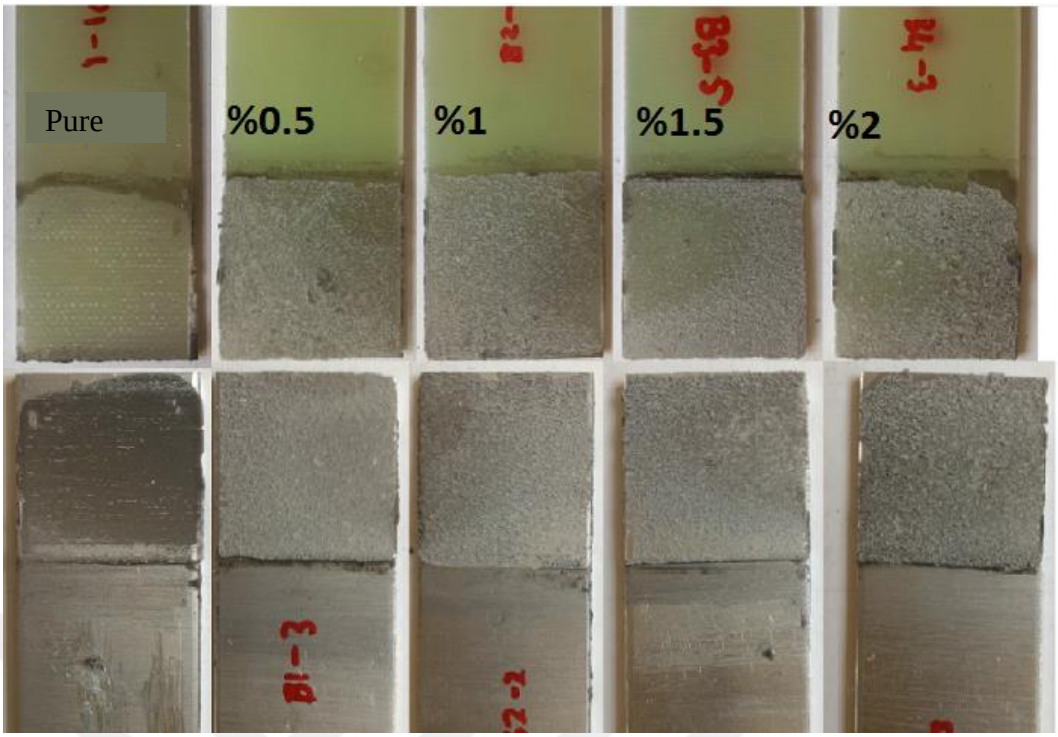

Figure 4.30 Views of samples after Mode V tensile test

4.5.2 Charpy Impact Test Results of Mode V Test

The results of the Charpy impact tests (average impact energy and impact toughness values) are given in Table 4.9 as the results obtained by Al side striking and in Table 4.10 as the results obtained by GFRP side striking.

Table 4.9 Charpy impact test results of nano-clay doped adhesive joints (Al side)

Adhesive type	Impact Energy (Joule)					Mean Impact Energy (Joule)	Impact Toughness a_{cu} (kj/m^2)
	Sample No						
	1	2	3	4	5		
Pure Araldite	3.6	3.3	3	4.3	3.5	3.54	15.32
0.5% Clay	3.7	3.5	3.8	4.0	3.9	3.78	16.36
1.0 % Clay	3.8	3.9	4.0	3.9	4.0	3.92	16.97
1.5 % Clay	3.8	3.9	4.0	3.7	4.0	3.88	16.80
2.0 % Clay	3.5	3.6	3.3	3.7	3.9	3.60	15.58

Table 4.10 Charpy impact test results of nano-clay doped adhesive joints (GFRP side)

Adhesive type	Impact Energy (Joule)					Mean Impact Energy (Joule)	Impact Toughness a_{cu} (kj/m^2)
	Sample No						
	1	2	3	4	5		
Pure Araldite	4.3	4.3	4.3	3.6	3.6	4.02	17.40
0.5% Clay	4.2	4.0	4.2	4.1	4.0	4.10	17.75
1.0 % Clay	4.7	4.7	4.5	4.6	4.4	4.58	19.83
1.5 % Clay	3.1	3.6	3.8	3.8	3.7	3.60	15.58
2.0 % Clay	4.5	3.0	3.2	2.1	4.0	3.36	14.55

Looking at the results obtained by striking in the Al side (Table 4.9), nano-clay addition up to 1.5% by wt. improves the toughness of the adhesive. The maximum impact energy was obtained as 3.92 joules with an increase of 10.7% in 1% nano-clay doped samples. It started to decrease after 1.5% (see Figure 4.31).

In the experiments made by GFRP side striking, the impact energy of 1% nano-clay doped samples increased by 13.9% (Table 4.10). However, addition of 1.5% and more nano-clay reduces the absorbed impact energy (Figure 4.31).

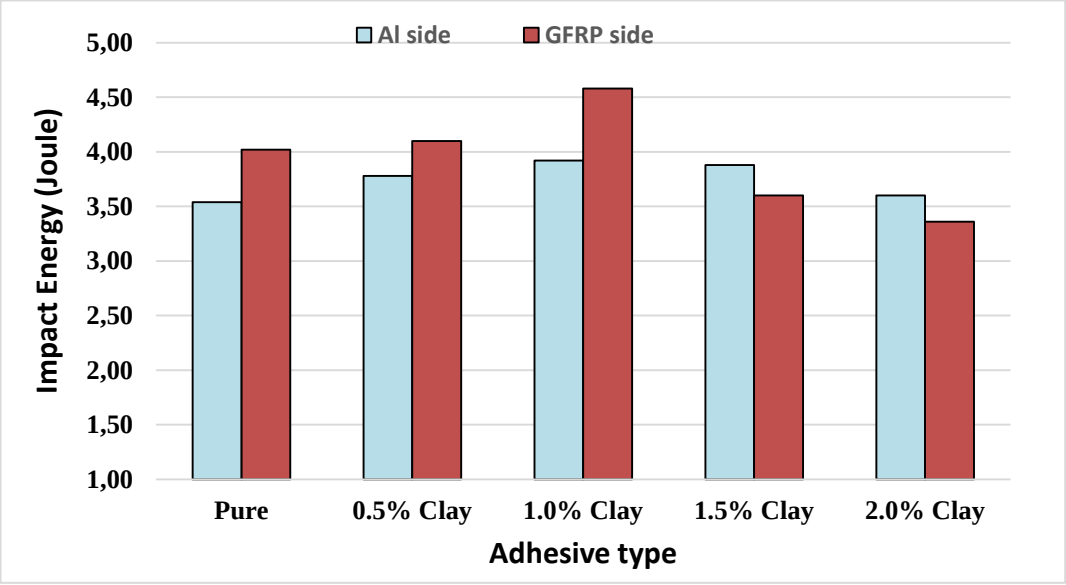

Figure 4.31 Charpy impact energy vs Al and GFRP side striking for Mode V test

In Figure 4.32 “G” label means GFRP plate is on the front, “PG” means unadulterated samples, “B” label means Al plate is on the front, and “BG1, BG2,

BG3 and BG4" means 0.5%, 1.0%, 1.5% and 2.0% by wt. nano-clay added samples, respectively.

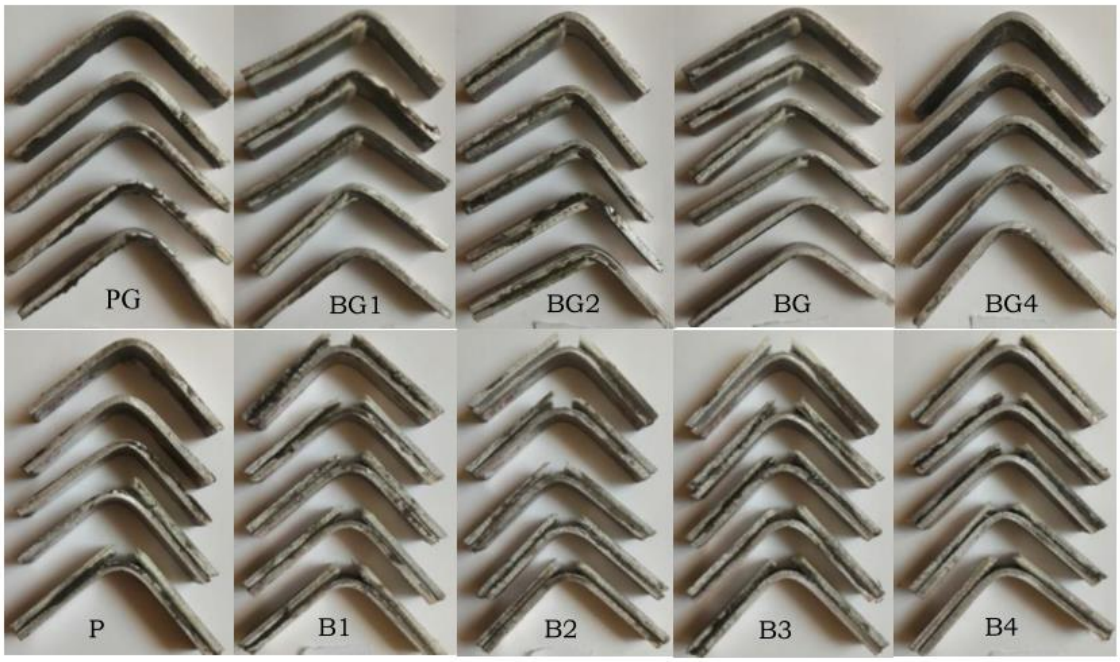

Figure 4.32 View of samples after Charpy impact test of nano-clay doped samples

In general, Al plates showed less plastic deformation in experiments with GFRP plates at the front (Figure 4.32 from BG1 to BG4), and it was seen that the bonds are broken in experiments with pure adhesive (Figure 4.32 P and PG). In experiments where Al-plate was on the front (Figure 4.32 B1, B2, B3, B4 and B5), adherent plates were not separated from each other, but in GFRP plate, due to resulting from tension after impact; it was observed that there was damage in the form of internal structure damage, fibre breakage and delamination (Figure 4.33).

At the experiments where GFRP plate is on the front, while GFRP parts were fully broken (separated) at unadulterated joints (Figure 4.34-a), only half of the GFRP part was separated from joint at nano-clay doped samples (Figure 4.34-b).

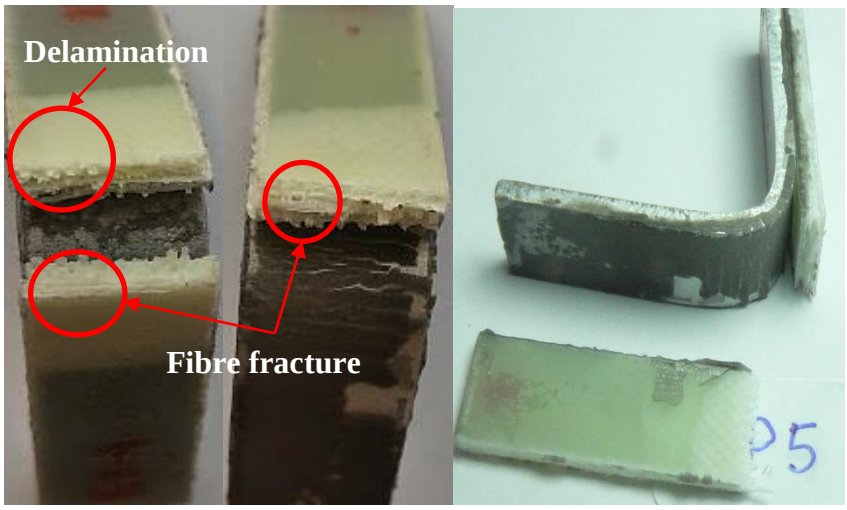

Figure 4.33 Damage views of nano-clay doped specimens after impact test (Al is on the front)

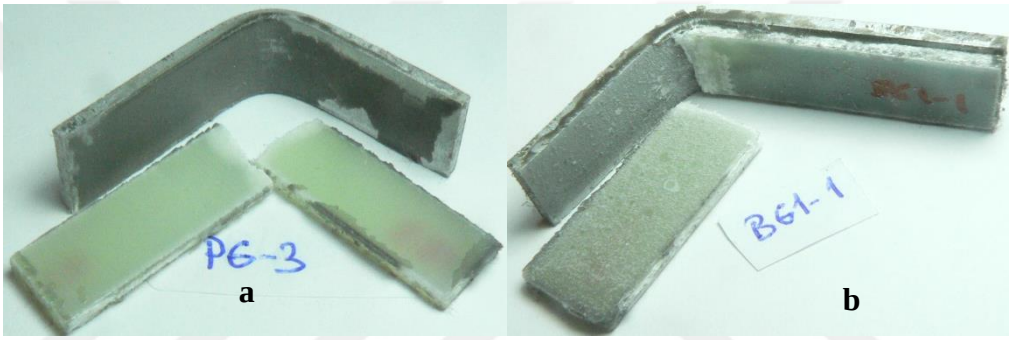

Figure 4.34 Damages when GFRP plate is on the front a) with pure Araldite b) nano-clay doped joints

CHAPTER 5

CONLUSIONS

In this thesis, the effects of adding nano-particles such as nano-silica, nano-clay and multi-walled carbon nano-tubes (MWCNT) to commercial epoxy adhesive (Araldite 2014) on the shear and impact strength of Al-GFRP single-lap joints were investigated. Shear performance of bonding samples were researched by universal tensile test machine in accordance to ASTM D 3039 international standards. In addition to this, Charpy impact test was used to evaluate the impact performances of samples in accordance to ISO 179 international standards.

The summary of the results obtained after tensile and Charpy tests are given below.

Mode I – II Tests:

- Adherents (Aluminum and glass fibre composites) must be adequately prepared before bonding in order to have higher bonding strengths.
- When the ashesion surfaces of the samples are examined after the tests, it is seen that there is no full bonding in the plates bonded with Araldite 2014-1, and almost all of the adhesive remains on one surface. Carbon Kleber CG-49 adhesive remain to both surfaces on the samples, and most of the samples were scraped from the composite surface.
- In experiments with Araldite 2014-1 adhesive, it was observed that the samples with 15mm overlap distance were more loaded and the ratio decreased as the overlap distance increased.

Again, the maximum shear strength was observed in the samples with the 15 mm overlap applied by this adhesive, and it was observed that as the overlap increased, this ratio decreased by 42%, 89%, and 159%.

- The maximum force is seen at 15 mm overlap distance for samples applied with Araldite 2014-1 adhesive, whereas at 30 mm overlap distance for samples applied with Carbon Kleber CG-49 adhesive.
- It is seen that samples prepared with Carbon Kleber CG-49 adhesive have higher loads as the lap distance increases and the highest load resistance is in the samples of C-30 series. The tensile strength was observed in the highest C15 series, while the tensile strength increased by 5%, 21%, 40%.
- The maximum force is in the C30 series applied to Carbon Kleber CG-49 when compared to the maximum tensile forces of the adhesives. It was observed to be 87% higher than that of the A15 series applied to Araldite 2014-1. When the shear strengths of adhesives are compared, it is observed that the shear strengths in the C15 series are 32% higher than the A15 series.
- It has been observed that the adhesive strength in some samples bonding is higher than the sample strength, however, the strength is also related to the thickness of metal, application force, and thickness of adhesive.
- In the comparison of Araldite 2014-1 and Carbon Kleber CG-49 adhesives, it was determined that the Carbon Kleber CG-49 type epoxy adhesive bonding have higher strength.
- Adhesive bonding, which has the same adhesive and overlap, can give different results due to the difference in adherents.

- Spew formation was observed in some of the samples that completed the curing time outside of the mold, while spew formation was observed in the mold cured. Spew formation should be eliminate before tests.
- These tests have been extensively demonstrated that the uniform distribution of nano-particles in the adhesive is a parameter that greatly influences the test results.
- When the results in Mode II are compared; It was observed that 0.5% nano-clay and nano-silica gave the highest result, while nano-particle ratio increased the tensile strength decreased. This indicates that the nano-particles are agglomerated in the adhesive due to poor dispersion and this adversely affect the bonding strength.
- The adhesive MWCNTs were added in amounts of 0.25%, 0.5%, 1%, 1.5%, and 2% by weight and the strength values increased by 47.7%, 62.2%, 48.1%, 33.8% and 21.5%, respectively.
- In MWCNT reinforced connections, the maximum average tensile strength was 8479.72 N and the average shear strength was measured to be 13.57 MPa. The maximum improvement was 62.2%.
- The average tensile strength was 5227.5 N and the average shear strength was 8.4 MPa at the joints bonded with neat Araldit 2014 adhesive.
- The bonding made by adding nano-clay in the adhesive at 0.5%, 1%, 1.5%, and 2% by weight increases the strength by 25.6%, 35.0%, 37.8% and 32.2%, respectively.
- The best strength in the nano-clay particle reinforced bonding is 1.5% by weight, with an average tensile strength of 7203.3 N and a shear strength of 11.5 MPa. The maximum bond strength is increased by 37.8%.

- The strength of the nano-silica additive bonding by weight was increased by 20.1%, 33.2%, 43.3% and 30.6%, respectively, for 0.5%, 1%, 1.5%, and 2%.
- The best strength in nano-silica additive bonding is 1.5% by weight, with an average tensile strength of 7490.8 N and a shear strength of 12.0 MPa. The maximum bond strength is increased by 43.3%.
- In general, experimental studies show that the nano-particles added to the commercial adhesive Araldite 2014-1 improve the tensile and shear resistance of Aluminum-GFRP single-bond adhesive bonding.
- When the samples are visually inspected after the tensile tests, the difference in rupture between the surfaces where the neat adhesives and the additive adhesives are applied is remarkable.
- It has been observed that the ruptures in the neat adhesive applied samples are due to adhesion. It is understood that the nano-clay additive bonding joints are from cohesion.
- The nano-particles ensure that the epoxy adhesive is better adhered to the aluminum and GFRP plates.
- These ratios can be taken as limit values since more than 1.5% by weight of nano-clay and nano-silica additive particles add up to 1.5% by weight and more than 0.5% by weight of additive particles lead to agglomeration of the particles.

After the Charpy impact tests, the following results were obtained:

- The fact that the front plate is made of Al or glass fibre significantly affects the damage caused by the impact energy and impact of the connection.
- The impact energy absorbed by the impact direction varies.

- The best ratio is 1% with increasing the impact energy of the 0.5% -1% nano-clay additive. More than 1% of the nano-clay addition reduces the toughness of the adhesive.
- On the one hand, it has been found that, in the case of neat adhesive joints, in general, the connection is broken and the plates are separated from each other. On the other hand, in connections made with a nano-clay added adhesive; It was seen that the links in the case where the Al plate was on the front did not break. In the case of GFRP front, it is seen that the single side of the glass fibre plates is broken in 0.5% and 1.5% additive additives.
- Experiments with glass fibre orientation showed that the addition of 1% nano-clay increased impact energy by 13.9%, and in experiments with Al plate, it increased by 10.7%.
- In the tests carried out on the Al front, the impact energy was increased by maximum of 3% at 1.5% by weight of the nano-silica connections, although the addition of the nano-silica particles did not significantly affect the bond strength.
- When the glass fibre was at the front, the absorbed impact energy and the ductility of the joints were improved by 1%, 3.5% and 10.9% respectively in the 0.5%, 1 %, 1.5% nano-silica added joints.
- The best ratio is 1.5% with increasing the impact energy of the 0.5% - 1.5% nano-silica additive bond. More than 1.5% of the nano-silica additive reduces the toughness of the adhesive.
- Al plates have undergone plastic deformation during the impact and permanent deformations have been observed on the plates after the tests. However, when impact is applied by glass fibre plates, the fibres absorb a

small portion of the impact energy. Thus, it seems that the bonding benefits the deformation of the aluminium plates.

- In all experiments, the glass fibres exposed to the impact were not able to carry the impact energy and were damaged due to the plastic deformations on the aluminium plate.
- In neat adhesive joints, it has been found that the joint is usually subjected to adhesion failure, and the plates are separated from each other. On the other hand, in the nano-silica additions, it can be seen that when the Al plate is at the front, the connections are not broken, and at the connections where the glass fibres are at the front, the single side of the glass fibre plates is broken with 0.5% and 1.5% additives. Moreover, the damage is observed as cohesion

5.1 Future Works

This study shows that adding nanoparticles to the adhesive in general improves the adhesive strength. Subsequent studies can explore the effects of adding more different nanoparticles. It is also possible to investigate how the mechanical properties of Al-Al, GFRP-GFRP or other metals like steel and other composite plates can be affected.

REFERENCES

[1] Pukanszky, B., Fekete, E. (1999). Advanced Polymer Science, **139**, 53-109

[2] Loctite Corporation 1996/1997 Edition (1995). *Loctite Worlwide Design Handbook*

[3] Loctite Corporation (1998). On CD. *Loctite Worlwide Design Handbook Second Edition*

[4] Kinloch, A.J. Little, M.S.G., and Watts, J.F. (2000). The Role of the Interphase in the Environmental Failure of Adhesive Joints, *Acta Materialia*, **48,** 4543-4553

[5] Yarrington, P., Zhang, J., Collier, C., and Bednarcyk, B.A. (2005). Failure Analysis of Adhesively Bonded Composite Joints. *American Institute of Aeronautics and Astronautics*, 1-23

[6] Papanikos, P., Tserpes, K.I., and Pantelakis, S. (2007). Innovation and Progression of Composite Patch Debonding in Adhesively Repaired Cracked Metallic Sheets. *Composite Structures*, **81,** 303-311

[7] Wahab, M.M.A. (2012). Fatigue in Adhesively Bonded Joints, *ISRN Materials Science*

[8] ASM (1990). *Adhesives and Sealants*, Engineered Materials Handbook vol. 3, The Materials International Society

[9] Adams, R. D., and Camyn, J. (2000). Joining Using Adhesives. *Assembly Automation*, **20,** 109-117

[10] Lees, W. A. (1989). *Adhesives and the Engineer*. National Starch & Chemical (Firm). Permabond Division

[11] Kinloch., A.J. (1997). Adhesives in Engineering. *Proceeding of the Institution of Mechanical Engineers*, **211,** 307-335

[12] Kinloch., A.J. (1987). *Adhesion and Adhesives Science and Technology*, Champman and Hall

[13] Müller, M., Hrabě, P., Chotěborský, R. & Herák, D. (2006). Theory of the Bonded Joint Creation Evaluation of Factors Influencing Adhesive Bond Strength. *Bonding Technology,* **52,** 30–37

[14] Gediktaş, M. (1984). *Bağlama Elemanları-Konstrüksiyon ve Hesap*, İTÜ Matbaası, İstanbul

[15] Higgins, A. (2000). Adhesive Bonding of Aircraft Structures. *International Journal of Adhesion and Adhesives*, **20**, 367–376

[16] Grant, L. D. R, Adams, R. D., and da Silva, L. F. M. (2009). Adhesive Bonding of Aircraft Structures. *International Journal of Adhesion and Adhesives,* **29,** 405–413.

[17] Effect, T. H. E., (2007). Yapıştırma bağlantılarının dayanımı üzerine kürleme basıncının etkileri, 470–479

[18] Gültekin, K. Ş., Akpinar, S. and Özel, A. (2015). The Effect of Moment and Flexural Rigidity of Adherend on the Strength of Adhesively Bonded Single Lap Joints. *The Journal of Adhesion,* **91:8,** 637-650

[19] Reis, P. N. B., Ferreira, J. A. M., and Antunes, F. (2011). Effect of Adherent's Rigidity on the Shear Strength of Single Lap Adhesive Joints. *International Journal of Adhesion and Adhesives,* **31,** 193–201

[20] Pinto, A. M. G., Campilho, R. D. S. G., Mendes, I. R., and Baptista, A. P. M. (2014). Effect of Adherend Recessing on the Tensile Strength of Single Lap Joints. *International Journal of Adhesion and Adhesives,* **90,** 89–103

[21] Aydin, M. D., Ozel, A., and Temiz, S., (2005). The Effect of Adherens Thickness on the Failure of Adhesively Bonded Single-Lap Joints. *Journal Adhesion Science Technology*, **19**, 705–718

[22] Cao, J., and Grenestedt, JL. (2004). Design and Testing of Joints for Composite Sandwich to Steel Hybrid Ship Hulls, *Composites,* **35**, 1091–105

[23] Kim, HS., and Lee, DG. (2005). Optimal Design of the Press Fit Joint for a Hybrid Aluminium to Composite Drive Shaft. *Composite Structures,* **70**, 33–47

[24] Lee, DG., Kim, HS., Kim, JW., and Kim, JK. (2004). Design and Manufacture of an Automotive Hybrid Aluminium to Composite Drive Shaft. *Composite Structures*, **63**, 87–99

[25] Cho, DH., and Lee, DG. (1997). Manufacture of One-Piece Automotive Drive Shafts with Aluminium and Composite Materials. *Composite Structures*, **38**, 309–319

[26] Chang., SH., Kim, PJ., Lee, DG., and Choi, JK. (2001). Steel to Composite Hybrid Headstock for High-Precision Grinding Machines. *Composite Structures*, **53**, 1–8

[27] Lee, CS., and Lee, DG. (2004). Manufacturing of Composite Sandwich Robot Structures Using the Co-Cure Bonding Method. *Composite Structures*, **65**, 307–18

[28] Mouritz, AP., Gellert, E., Burchill, P., and Challis, K. (2001). Review of Advanced Composite Structures for Naval Ships and Submarines. *Composite Structures*, **53**, 21–41

[29] Zitoune, R., and Collombet, F. (2007). Numerical Prediction of the Thrust Force Responsible of Delamination During the Drilling of the Long-Fibre Composite Structures. *Composites*, **38**, 858–66

[30] Davim, JP., Reis, P., and Antonio, CC. (2004). Experimental Study of Drilling Glass Fibre Reinforced Plastics (GFRP) Manufactured by Hand Lay-Up. *Composite Science Technology*, **64**, 289–97

[31] Tjong, S.C., (2006). Structural and Mechanical Properties of Polymer Nanocomposites. *Material Science and Engineering R. Reports*, **53**, 73-197

[32] Pavlidou, S., and Papaspyrides, C.D. (2008). A Review on Polymer-Layered Silicate Nano-Composites. *Progress in Polymer Science*, **33**, 1118-1119

[33] Azeez, A.A., Rhee, K.Y, Park, S.J., and Hui, D. (2013). Epoxy Clay Nanocomposites Processing, Properties and Applications. *Composites*, **45**, 308-320

[34] Sancaktar, E., and Kuznicki, J. (2011). Nanocomposite Adhesives: Mechanical Behaviour with Nanoclay, *International Journal of Adhesion and Adhesives*, **31**, 286-300

[35] Chavooshiana, M., Kamalia, R., Tutunchi, A., and Kianvash A. (2017). Effect of Silicon Carbide Nanoparticles on the Adhesion Strength of Steel to Epoxy Composite Joints Bonded With Acrylic Adhesives. *Journal of Adhesion Science and Technology*, **31**, 345–357

[36] Zielecki, W., Kubit, A., Trzepiecinski, T., Narkiewicz, U. and Czech, Z. (2017). Impact of Multiwall Carbon Nanotubes on the Fatigue Strength of Adhesive Joints. *International Journal of Adhesion and Adhesives*, **73**, 16–21

[37] Zhang, J., Luo, R. and Yang, C. (2012) A Multi-Wall Carbon Nanotube-Reinforced High-Temperature Resistant Adhesive for Bonding Carbon to Carbon Composites, *Carbon N. Y.*, **50**, 4922–4925

[38] Yu, S., Tong, M. N. and Critchlow, G. (2010). Use of Carbon Nanotubes Reinforced Epoxy as Adhesives to Join Aluminum Plates. *Materials and Design*, **31**, 126-129

[39] Wernik, J. M. and Meguid, S. A. (2014). On the Mechanical Characterization of Carbon Nanotube Reinforced Epoxy Adhesives. *Materials and Design*, **59,** 19–32

[40] Vietri, U., Guadagno, L., Raimondo, M., Vertuccio, L. and Lafdi, K. (2014). Nanofilled Epoxy Adhesive for Structural Aeronautic Materials. *Composites*, **61,** 73–83

[41] Sydlik, S. A., Lee, J. H., Walish, J. J., Thomas, E. L. and Swager, T. M. (2013). Epoxy Functionalized Multi-Walled Carbon Nanotubes for Improved Adhesives. *Carbon N. Y.* **59,** 109–120

[42] Akpinar, I. A., Gültekin, K., Akpinar, S., Akbulut, H. and Ozel, A. (2017). Experimental Analysis on the Single-Lap Joints Bonded by a Nanocomposite Adhesives Which Obtained by Adding Nanostructures. *Composites*, **110,** 420–428

[43] Ayatollahi, M. R., Giv, A. N., Razavi, S. M. J. and Khoramishad, H. (2016). Mechanical Properties of Adhesively Single Lap-Bonded Joints Reinforced with Multi-Walled Carbon Nanotubes and Silica Nanoparticles. *Journal of Adheives*, **0,** 1–18

[44] Yu, S., Tong, M. N. and Critchlow, G. (2010). Use of Carbon Nanotubes Reinforced Epoxy as Adhesives to Join Aluminum Plates. *Materials and Design*, **31,** 126-129

[45] Tutunchi, A., R. Kamali, and A. Kianvash (2015). Adhesive Strength of Steel to Epoxy Composite Joints Bonded with Structural Acrylic Adhesives Filled with Silica Nanoparticles. *Journal of Adhesion Science and Technology*, **29**, 195–206

[46] Hsieh, T.H., Liang, C.H. (2014). Improvement of Impact-Absorbed Energy of CFRPs on Adding the Nanoparticles Into Epoxy Resins. *Journal of Chemistry and Chemical Engineering*, **8**, 692-697

[47] Nassar, S.A., A. Z. Wu, K. Moustafa and D. Tzelepis (2015). Effect of Adhesive Nanoparticle Enrichment on Static Load Transfer Capacity and Failure Mode of Bonded Steel to Magnesium Single Lap Joints. *Journal of Manufacturing Science and Engineering*, **137**, 1-6

[48] Zhou, H., H.Y. Liu, H. Zhou, Y. Zhang, X. Gao and Y. W. Mai (2016). On Adhesive Properties of Nano-Silica/Epoxy Bonded Single-Lap Joints. *Materials and Design*, **95**, 212–218

[49] Meng, Q., Wang, C.H., Saber, N., Kuan, H.-C., Dai, J., Friedrich, K., and Ma, J., (2014). Nanosilica-Toughened Polymer Adhesives. *Materials and Design,* **61,** 75–86

[50] Zhou, H., Liu, HY., Zhou, H., Zhang, Y., Gao, X., and Mai, YW., (2016). On Adhesive Properties of Nano-Silica/Epoxy Bonded Single-Lap Joints. *Materials and Design*, **95,** 212–218

[51] Sinha Ray, S. and Okamoto, M. (2003). Polymer/Layered Silicate Nanocomposites: A Review From Preparation to Processing. *Progress in Polymer Science*, **28**, 1539–1641

[52] Gu, A. and Liang, G. (2003). Thermal Degradation Behaviour and Kinetic Analysis of Epoxy/Montmorillonite Nanocomposites. *Polymer Degradation and Stability*, **80**, 383–391

[53] Khalili, S. M. R., Tavakolian, M., Sarabi, A. (2010). Mechanical Properties of Nanoclay Reinforced Epoxy Adhesive Bonded Joints Made with Composite Materials. *Journal of Adhesion Science and Technology*, **24**, 1917–1928.

[54] Reis, P.N.B., Ferreira, J.A.M., Santos, P., Richardson, M.O.W., and Santos, J.B. (2012). Impact Response of Kevlar Composites with Filled Epoxy Matrix. *Composite Structures*, **94**, 3520–8

[55] Rafiq, A., Merah, N., Boukhili, R., and Al-Qadhi, M. (2017). Impact Resistance of Hybrid Glass Fibre Reinforced Epoxy/Nanoclay Composite. *Polymer Testing*, **57**, 1-11

[56] Jeyakumar, R., Sampath, P. S., Ramamoorthi, R. and Ramakrishnan, T. (2017). Structural, Morphological and Mechanical Behaviour of Glass Fibre Reinforced Epoxy Nanoclay Composites. *International Journal Advanced Manufecturing Technologies*, **93**, 1-9

[57] Galimberti, M., Cipolletti, V. R. and Coombs, M. (2013). Applications of Clay–Polymer Nanocomposites. *Handbook of Developes in Clay Science*, **5**, 539-586

[58] Goudarzia, R.H. and M.R. Khedmati (2015). An Experimental Investigation of Static Load Capacity of AL-GFRP Adhesively Bonded Single Lap and Souble Butt Lap Joints. *Latin American Journal of Solids and Structures*, **12**, 1583-1594

[59] Saldanha, D.F.S., Canto, C., Dasilva, L.F.M, Carbas, R.J.C. Chaves, F.J.P., Nomurac, K., and Ueda, T., (2013). Mechanical Characterization of a High Elongation and High Toughness Epoxy Adhesive. *International Journal of Adhesion and Adhesives*, **47**, 91–98

[60] Silva, L.F.M., Öchsner, A., and Adams, R.D. (2011). *Handbook of Adhesion Technology*. Introduction to Adhesive Bonding Technology, 1st ed. Berlin, Springer

[61] Hersam, M. (2008). Progress Towards Monodisperse Single-Walled Carbon Nanotubes. *Nature Nano*, **3**, 387-394

[62] Bell, A. and Kinloch, A. (1997). The Effect of the Substrate Material on the Value of the Adhesive Fracture Energy. *Journal of Materials Science Letters*, **16**, 1450-14